Environment Canada

Environnement Canada

Transient Response of Shallow Enclosed Basins Using the Method of Normal Modes

Desiraju B. Rao *

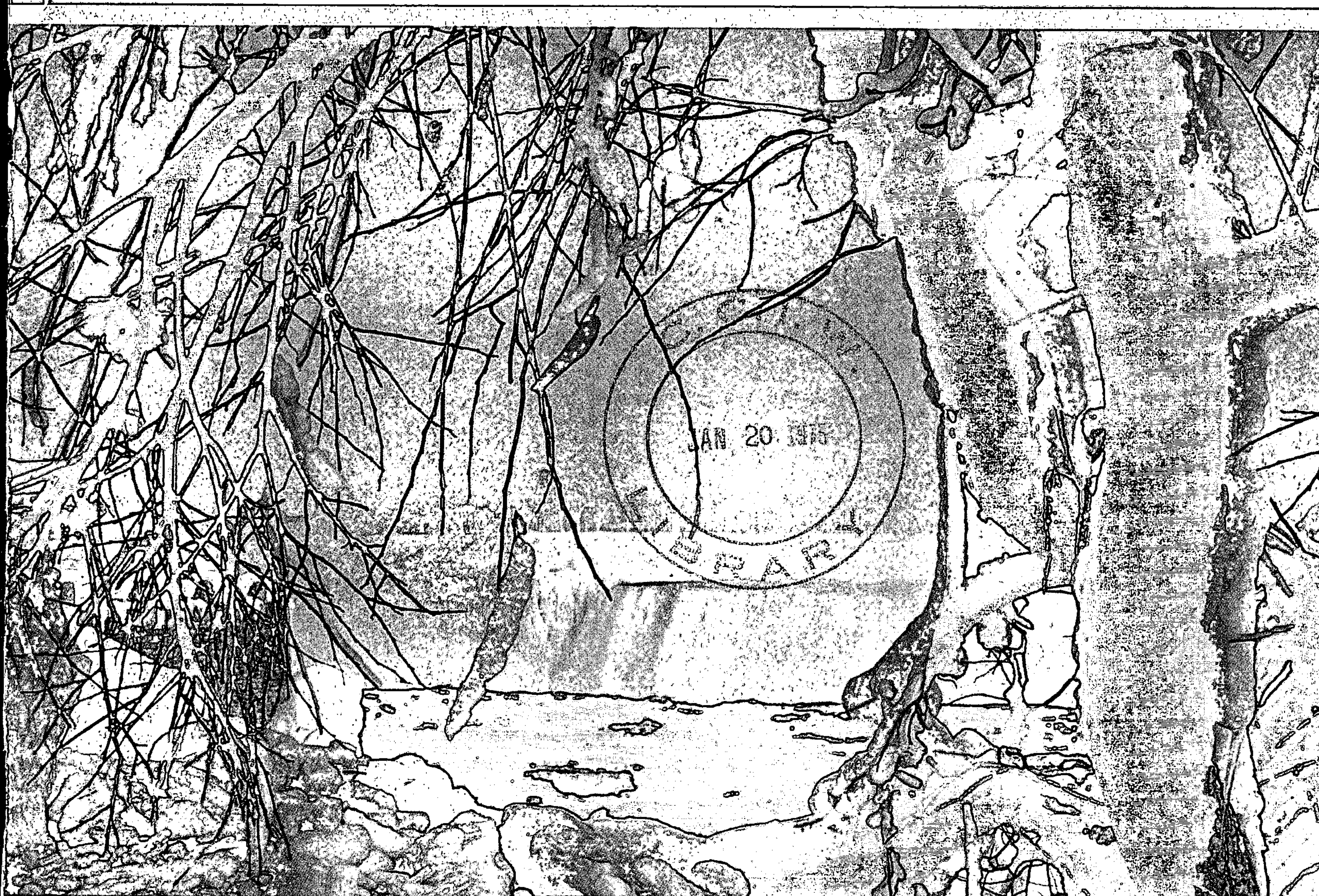

SCIENTIFIC SERIES NO. 38
(Résumé en français)

INLAND WATERS DIRECTORATE,
CANADA CENTRE FOR INLAND WATERS,
BURLINGTON, ONTARIO, 1974

Environment Canada Environnement Canada

Transient Response of Shallow Enclosed Basins Using the Method of Normal Modes

Desiraju B. Rao *

*Present affiliation: Department of Energetics and the Center for Great Lakes Studies, the University of Wisconsin-Milwaukee, Milwaukee, Wisconsin 53201.

SCIENTIFIC SERIES NO. 38
(Résumé en français)

INLAND WATERS DIRECTORATE,
CANADA CENTRE FOR INLAND WATERS,
BURLINGTON, ONTARIO, 1974

Cat. No.: En 36-502/38

CONTRACT NO. KL327-4-8069
THORN PRESS LIMITED

Contents

	Page
ACKNOWLEDGEMENTS	v
ABSTRACT	vii
RÉSUMÉ	vii
GENERAL CONSIDERATIONS	1
1. Introduction	1
2. Dynamic equations	3
3. Normal modes of an arbitrary basin	4
4. Forced solution	8
Method I	8
Method II	10
Finite difference integrations	12
EXAMPLES OF FORCED OSCILLATIONS	14
(A) Disturbance propagating over a non-rotating basin of uniform depth	14
5. Normal modes	14
6. Forced solution	15
7. Results	18
(B) Stationary disturbance over a rotating basin of uniform depth	22
8. Construction of the orthogonal functions	22
9. Forced solution	22
10. Results	23
SUMMARY	29
REFERENCES	30

Illustrations

Figure 1. A schematic diagram of the rectangular basin with the stress band approaching from an angle θ	16
Figure 2. Various epochs of time as the stress band crosses the basin	16
Figure 3. Comparison of spectral solution (solid line) with the exact solution for $\theta = 0$, $V = 0.5$, and $b/a = 5$	17
Figure 4. Water level fluctuations at points $x = -a$, $y = 0$ (LL); $x = a$, $y = 0$ (LR); $x = -a$, $y = b$ (UL); $x = a$, $y = b$ (UR); as a function of time for $\theta = \pi/6$, $V = 0.5$ in a square basin	19

Illustrations (cont.)

	Page
Figure 5. Water level fluctuations at points $x = -a$, $y = 0$ (LL); $x = a$, $y = 0$ (LR); $x = -a$, $y = b$ (UL); $x = a$, $y = b$ (UR); as a function of time for $\theta = \pi/3$, $V = 0.5$	19
Figure 6. Water level fluctuations at points $x = -a$, $y = 0$ (LL); $x = a$, $y = 0$ (LR); $x = -a$, $y = b$ (UL); $x = a$, $y = b$ (UR); as a function of time for $\theta = \pi/6$, $V = 1.5$	20
Figure 7. Water level fluctuations at points $x = -a$, $y = 0$ (LL); $x = a$, $y = 0$ (LR); $x = -a$, $y = b$ (UL); $x = a$, $y = b$ (UR); as a function of time for $\theta = \pi/3$, $V = 1.5$	20
Figure 8. Water level fluctuations *vs.* time at various points on the boundary of a rotating rectangular basin	25
Figure 9. Location of the nodal line in the (x,y)-plane at various instants of time for parameter values given in Figure 8	25
Figure 10. Water level fluctuations on the southern boundary ($y = 0$) as a function of time for $f = 0.12$, $\lambda = 10^{-2} \times f$, $b/a = 0.5$ with a uniform wind stress in the positive x-direction	27
Figure 11. Nodal line configuration at various instants of time for parameter values given in Figure 10	27

Tables

1. Maximum and minimum water levels as a function of V and θ for a square basin . . . 21
2. Maximum and minimum water levels as a function of V and θ for a basin having north-south length two and a half times the east-west length . . . 21
3. Height values (cm) on the southern boundary from spectral and finite-difference methods at approximately $t = 0.5$ T . . . 26

Acknowledgements

A large part of the calculations and the writing of this report were supported by contract from the Canada Centre for Inland Waters, Burlington, Ontario. I am much indebted to Dr. T. J. Simons of CCIW for several discussions, suggestions, and a critical review of the manuscript. The help of Mr. Hilton Steves of the Marine Sciences Directorate, Department of the Environment, Ottawa, Miss Nancy Smith, and particularly Mr. Manuel Nunez of CCIW in programming the calculations is gratefully acknowledged.

Abstract

Predicting the two-dimensional forced response (or the storm surge) of an arbitrary water body is discussed in terms of the normal mode expansion technique. Such an approach eliminates space dependence from the governing equations. Time-dependent aspects of the problem may then be solved either by a numerical evaluation of a formal integral solution, which involves the normal mode functions and the wind stress field, or by a direct finite-difference integration in time alone by some explicit or implicit schemes. Hence the use of normal mode expansion procedure eliminates a complete numerical integration of the problem on a space-time finite difference grid, and offers certain advantages in avoiding such problems as computational stability, grid-dispersion, etc. A method is described for constructing the quasi-static normal modes for an arbitrary rotating basin and different methods are presented for obtaining the general solution for the forced response. Application of some of these procedures to two ideal cases is then considered. One case deals with the response of a non-rotating rectangular basin of uniform depth to a semi-infinite stress band propagating across the basin in a given direction; the other deals with the effect of an instantaneously imposed wind stress on a rotating rectangular basin of uniform depth.

Résumé

On traite de la prévision d'une réponse forcée bi-dimensionnelle (ou soulèvement de tempête) d'une masse d'eau imaginaire en termes de la technique d'expansion en mode normal. Une approche de ce genre élimine la dépendance d'espace des équations gouvernantes. Les aspects du problème qui sont subordonnés au temps peuvent alors être résolus soit par l'évaluation numérique d'une solution formelle intégrale qui implique les fonctions en mode normal et le champ de tension du vent, soit par l'intégration directe au moyen de la différence finie dans le temps uniquement au moyen de schémas explicites ou implicites. Par conséquent, l'emploi du procédé d'expansion en mode normal élimine l'intégration numérique complète du problème au moyen d'un quadrillage temps-espace de différence finie et présente certains avantages en écartant les problèmes de stabilité des calculs, de dispersion du quadrillage, etc. On décrit une méthode de construction de modes normaux quasi-statiques en ce qui concerne un bassin rotatif imaginaire, en plus de différentes méthodes pour obtenir la solution générale à la réponse forcée. On étudie alors la possibilité d'appliquer quelques-uns de ces procédés dans deux cas idéaux. Le premier porte sur la réponse d'un bassin rectangulaire non rotatif et de profondeur uniforme à une bande de tension semi-infinie qui se propage d'un bout à l'autre du bassin dans une direction donnée, tandis que l'autre porte sur l'effet de la tension du vent imposée de façon instantanée sur un bassin rectangulaire et rotatif de profondeur uniforme.

CHAPTER 1

General Considerations

1. INTRODUCTION

The analytical theory of forced oscillations of a water body has generally been confined to the one-dimensional aspect. The response of the water body under the constraint of one-dimensionality has included disturbances that are uniform both in space and time, or uniform in space but amplitude changing in time (i.e., instantaneous forcing); or propagating disturbances in which the forcing function over the water body is dependent on both space and time (Lamb, 1932; Proudman, 1929; and Rao, 1967, 1969). Such one-dimensional studies explain some fundamental aspects of the forced oscillations.

In practice, however, the response of any water body to an arbitrary disturbance is at least two-dimensional (the entire horizontal plane). The analytical theory of the two-dimensional response of rectangular bays — that is, water bodies with one end open to a deep ocean — has been considered in a series of extensive investigations by Lauwerier (see Lauwerier and Damste, 1963 for a list of all references pertaining to this series). In these studies, Lauwerier considered basins that have uniform as well as variable depths, and disturbances that are uniform both in space and time, or those that only change in time with application of the results to the storm surges in the North Sea along the Dutch Coast.

This study deals with the general theory of two-dimensional response of a completely enclosed basin, e.g., a lake. In Chapter I the theory is presented of obtaining the solutions for the forced response of the basin by various methods that involve combinations of analytical-numerical considerations. In Chapter II the application of these methods to two ideal cases is described. Chapter III is a summary.

The methods described here, make use of the principle of representing the forced solution by an appropriate combination of the free (or characteristic or eigen) solutions of the basin, which automatically satisfy the necessary boundary conditions. Adopting this procedure eliminates the space-dependent aspect of the forced solution. The problem of determining the latter then reduces to solving a system of (either coupled or uncoupled) inhomogeneous, ordinary, differential equations of the first order, with time as the independent variable, for the expansion coefficients. In this respect, the procedure described here differs from that of Lauwerier (loc. cit.). In the latter's approach to the problem, the time-dependence in the governing equations is eliminated by using the Laplace-transform; the resulting system of equations essentially leads to an inhomogeneous elliptic equation. The problem then is solved by a superposition of the fundamental wave solutions in a rectangular geometry, namely the Poincaré and Kelvin waves. As these solutions satisfy the wave-equation but not all the boundary conditions, the expansion coefficients must then be determined to satisfy the latter requirement. This approach has one disadvantage, i.e., the Laplace-transform has to be inverted to obtain the solution. For arbitrary wind fields, the inversion procedure will, in general, be difficult and requires introduction of additional approximations (Lauwerier, 1961).

First a general method is described for determining the characteristic functions of an arbitrary basin. Traditionally, in the field of limnology, the normal modes of lakes and bays have been determined for one-dimensional channels (Platzman and Rao, 1964). Only recently have the two-dimensional aspects of lake oscillations started receiving attention. Loomis (1970) determined the two-dimensional normal modes for bays and harbours of Hawaii without considering the earth's rotation. Platzman (1971) obtained the fundamental modes for Lake Superior and the Gulf of Mexico, taking the earth's rotation into account by the method of resonance interactions. When several of the normal modes are required, as in the present case, Platzman's method becomes difficult to apply, requiring repeated searches for each mode.

Hence, in this study, a different approach is adopted, one that is capable of yielding several of the normal modes simultaneously. The solution is obtained through the decomposition of the vertically integrated flow into an irrotational part and a solenoidal part. The characteristic functions for each of the parts are obtained by solving the appropriate eigenvalue problem. This procedure is the same as the one used by Proudman (1916) and Rao (1966) to study problems of free oscillations of rotating basins; but here it is also extended to include arbitrary bottom friction law and external wind-stress force. The various methods of obtaining the forced solution are then discussed. The forced solution is obtained by finding the particular solution, which is determined by the forcing function, and by combining it with the homogeneous solutions, to satisfy the necessary initial conditions. One of the methods leads to a set of coupled ordinary inhomogeneous differential equations, which are obtained when the technique of Proudman for the study of free oscillations is extended to the forced case. Another method, in which an expansion technique, used by Reid (1958) in a study of edge wave resonance problems, is employed, leads to uncoupled inhomogeneous equations. In both these methods, the time dependent part of the solution may be represented formally for an arbitrary case by an integral overtime, which can be evaluated by Simpson's rule or any other standard method of evaluating integrals numerically. Finally, the solution to the time-dependent part by direct finite-difference integrations in time is also considered.

The problems discussed here may also be solved by direct finite-difference methods of integration both in space and time. Indeed, this is what is generally done for predicting storm surges on real water bodies such as the North Sea, Lake Erie, etc. (Platzman, 1963; Welander, 1961). This procedure requires a three-dimensional, space-time finite-difference mesh with proper staggering of the dependent variables. The time integrations are usually done by using explicit schemes with the attendant limitations on time increment imposed on the scheme by the chosen space-grid interval, to ensure computational stability. Furthermore, for arbitrary basins with irregular boundary configuration, problems of grid dispersion can be aggravating (Simons, 1971). In addition, when a prediction has to be made, direct finite-difference methods require starting the integrations more or less from scratch.

The storm surge prediction problem may also be approached, as described above, from the methodology of using the eigenfunctions of the basin. Such an approach has certain advantages over space-time finite-difference integrations, even if the eigenfunctions for a real basin have to be computed numerically, especially if a large number of predictions are to be made for the same region. (This, of course, is the case when any storm surge model is considered for an operational purpose). In most cases, the eigenfunction expansion converges rapidly. Also, because these functions can be computed once and for all for a given basin, the storm surge prediction problem simply reduces to solving ordinary inhomogeneous differential equations of the first order in time as described above. Even if these are solved by finite-difference methods (in preference to using the formal integral solution in time) one can use here implicit time integration schemes without any difficulty, as the governing equations are linear. Use of an implicit method permits the employment of larger time steps, as these methods are stable for any chosen time-increment; thereby the prediction problem becomes more economical from the point of view of the computer time used.

The ultimate purpose of this investigation is to apply the eigenfunction technique for storm surge predictions in the Great Lakes, e.g., Lake Ontario, and to test the efficiency and accuracy of these procedures with direct space-time numerical integrations conducted at the Canada Centre for Inland Waters. The method, in the preliminary stages, is tested on certain ideal cases in which the horizontal-plan form is taken as rectangular and the depth as uniform. A few of these results are presented.

2. DYNAMIC EQUATIONS

For the dynamic equations governing the response of a water body to an imposed disturbance, consider a body of water which is homogeneous. Take a right-handed Cartesian co-ordinate system having its origin at the mean surface level with x-axis pointing eastward, y-axis pointing northward, and z-axis pointing upward. Let H(x,y) denote the equilibrium depth of the water in the lake which is bounded by a horizontal boundary S(x,y). Assume that the water body is on a plane rotating about its vertical axis with a constant angular speed Ω. Further assume that the depth H is much less than the scale of horizontal disturbances in the lake, so that the shallow water approximation may be invoked. This assumption then permits us to replace the pressure-gradient terms in the horizontal momentum equations by their hydrostatic equivalents. By suppressing the non-linear advective terms in the momentum equations (based on the usual order of magnitude considerations), the vertically integrated equations of motion and mass conservation may be written as follows:

$$\frac{\partial \mathbf{M}}{\partial t} - f\,[\mathbf{M}] = -\,g\bar{H}h\,\nabla\zeta + \tau_S + \tau_B \tag{2.1}$$

$$\frac{\partial \zeta}{\partial t} + \nabla\cdot\mathbf{M} = 0 \tag{2.2}$$

In the above equations **M** is the transport vector

$$\mathbf{M} \equiv \int_{-h\bar{H}}^{\zeta} \mathbf{V}\, dZ \tag{2.3}$$

where $\mathbf{V} \equiv (u,v)$ is the horizontal velocity vector; [**M**] indicates a rotation of vector **M** through ninety degrees in the negative sense of the horizontal plane; ζ is the perturbation height of the water level, and is assumed to be small compared to the depth so that the pressure-gradient term may be linearized; h is a non-dimensional depth parameter defined by

$$h\,(x,y) \equiv \frac{H\,(x,y)}{\bar{H}} \tag{2.4}$$

where $\bar{H}$ is some constant mean depth. If one assumes that the water density ρ is unity, then τ_S and τ_B represent the wind stress vector at the surface and the bottom stress vector, respectively. $\nabla \equiv \left(\frac{\partial}{\partial x}, \frac{\partial}{\partial y}\right)$ is the horizontal gradient operator, $f \equiv 2\,\Omega \sin\theta$ is the coriolis parameter, and g is the constant of apparent gravitational acceleration.

In equation (2.1) the surface wind stress τ_S is in the nature of an external parameter which is prescribed, based on the atmospheric wind field. If the bottom stress vector τ_B can be prescribed (or parameterized) in terms of the unknown quantities, namely, the dependent variables, then equations (2.1) and (2.2) form a closed set of equations which may then be solved subject to the appropriate initial and boundary conditions. Neglecting the question of the difficulties associated with a proper parameterization, we assume here that τ_B, when it is taken into account, is given by

$$\tau_B = \lambda\,\mathbf{M} \tag{2.5}$$

where λ is an appropriate friction coefficient, which in principle can be depth dependent. Substitution of equation (2.5) into (2.1), closes the problem on the dependent variables **M** and ζ.

The boundary conditions appropriate to a totally enclosed water body like a lake are:

$$\mathbf{M}\cdot\mathbf{n} = 0 \quad \text{on the boundary} \tag{2.6}$$

where n represents the outward drawn unit normal vector to the boundary curve S(x,y). To focus attention only on the response produced by the wind stress forcing, an initial state of rest in the lake is assumed so that at time

$$t = 0 : \mathbf{M} = 0 \, ; \zeta = 0 \tag{2.7}$$

Now equations (2.1), (2.2) along with the conditions (2.6) and (2.7) pose an initial-boundary value problem of inhomogeneous nature, having a unique solution $\mathbf{M}(x,y,t)$ and $\zeta(x,y,t)$ corresponding to a prescribed forcing function $\tau_S(x,y,t)$.

3. NORMAL MODES OF AN ARBITRARY BASIN

Because the method used here is completely dependent on a knowledge of the normal modes, the question of how to determine them for an arbitrary basin is considered first. This requires, in principle, the solution of the characteristic value problem associated with (2.1), (2.2) and (2.6) (with $\tau_S = 0$). In general, for a real water body, this aspect of the problem will become rather complicated. If, for example, an attempt is made to solve this problem, by assuming that the normal modes are of the form

$$\mathbf{M} = \mathbf{M}(x,y)\, e^{i\sigma t}$$

$$\zeta = \zeta(x,y)\, e^{i\sigma t}$$

where σ is the frequency of oscillation and by eliminating $\mathbf{M}$ in the free equations, the result is (ignoring τ_B for the time being):

$$\nabla \cdot h \nabla \zeta + \frac{\sigma^2 - f^2}{g\bar{H}} \zeta - \frac{if}{\sigma} \nabla h \cdot [\nabla \zeta] = 0 \tag{3.1}$$

with the boundary condition

$$\frac{\partial \zeta}{\partial n} + \frac{if}{\sigma}\frac{\partial \zeta}{\partial s} = 0 \tag{3.2}$$

on the boundary. Here n and s are the normal (outward) and tangential (counter-clockwise) directions to the boundary curve. The characteristic values and functions are then obtained by solving the second order elliptic differential equation above. Even though the problem is now reduced to solving (3.1) and (3.2) involving a single scalar dependent variable, a disadvantage of the method is the appearance in (3.2) of the characteristic value σ, which itself is an unknown. A more convenient, if somewhat more elaborate, method of obtaining the free solutions, is now described in this section.

The transport field $\mathbf{M}$ is independent of depth and as the motion takes place in a basin completely enclosed by rigid boundaries on which $\mathbf{M} \cdot \mathbf{n} = 0$, $\mathbf{M}$ may be represented as

$$\mathbf{M} \equiv \mathbf{M}^{\phi} + \mathbf{M}^{\psi}$$

where $\mathbf{M}^{\phi}$ and $\mathbf{M}^{\psi}$ are given in terms of two scalar functions ϕ and ψ:

$$\mathbf{M}^{\phi} \equiv - h \nabla \phi \, ; \mathbf{M}^{\psi} = - [\nabla \psi] \tag{3.3}$$

ϕ and ψ are the potential and stream functions for the transport field. From (3.3) it can be seen that $\mathbf{M}^{\psi}$ represents the solenoidal part of $\mathbf{M}$ and $h^{-1} \mathbf{M}^{\phi}$ represents the irrotational part. That is,

$$\nabla \cdot [h^{-1} \mathbf{M}^{\phi}] = 0 \text{ and } \nabla \cdot [h^{-1} \mathbf{M}] = \nabla \cdot [h^{-1} \mathbf{M}^{\psi}] = + \nabla \cdot h^{-1} \nabla \psi \tag{3.4a}$$

$$\nabla \cdot \mathbf{M}^{\psi} = 0 \text{ and } \nabla \cdot \mathbf{M} = \nabla \cdot \mathbf{M}^{\phi} = -\nabla \cdot h \nabla \phi \tag{3.4b}$$

In order to satisfy the boundary condition $\mathbf{M} \cdot \mathbf{n} = 0$, it is required that

$$\mathbf{M}^{\phi} \cdot \mathbf{n} = 0 \;;\; \mathbf{M}^{\psi} \cdot \mathbf{n} = 0 \tag{3.5}$$

on the boundaries. The conditions (3.5) imply that

$$h \frac{\partial \phi}{\partial n} = 0 \;; \qquad \psi = 0 \tag{3.6}$$

on the boundary.

It can now be shown that $\mathbf{M}^{\phi}$ and $\mathbf{M}^{\psi}$ as defined by (3.3) and (3.5) determine uniquely the total transport field $\mathbf{M}$, that is,

$$\hat{\mathbf{M}} \equiv \mathbf{M} - (\mathbf{M}^{\phi} + \mathbf{M}^{\psi}) = 0$$

To prove the latter statement, it is first noted that $\nabla \cdot [h^{-1} \hat{\mathbf{M}}] = 0$ from (3.4a), so that, e.g., $h^{-1} \hat{\mathbf{M}} = -\nabla \hat{\phi}$. However, $\nabla \cdot \hat{\mathbf{M}} = 0$ from (3.4b); hence $-\nabla \cdot \hat{\mathbf{M}} = \nabla \cdot h \nabla \hat{\phi} = 0$. As the normal component of $\hat{\mathbf{M}} = 0$ on the boundary, so is that of $h \nabla \hat{\phi}$. It follows then that $\hat{\phi}$ = constant and $\hat{\mathbf{M}} = 0$.

The determination of $\mathbf{M}^{\phi}$ and $\mathbf{M}^{\psi}$ in terms of $\mathbf{M}$ proceeds by conversion of (3.3) into the inhomogeneous elliptic equations:

$$\nabla \cdot h \nabla \phi = -\nabla \cdot \mathbf{M}, \quad \nabla \cdot h^{-1} \nabla \psi = \nabla \cdot [h^{-1} \mathbf{M}] \tag{3.7}$$

with homogeneous boundary conditions (3.6). Since $\mathbf{M}$ itself is an unknown, but satisfies the dynamic equations, the governing equations are converted into conditions on ϕ and ψ, from which $\mathbf{M}$ is then reconstructed using (3.3). For this purpose, ϕ and ψ are represented in terms of the spectra of the elliptic operators appearing in (3.7). That is, the characteristic value problems are considered first:

$$\left.\begin{aligned} &\nabla \cdot h \nabla \phi_\alpha = -\lambda_\alpha \phi_\alpha \\ &h \frac{\partial \phi_\alpha}{\partial n} = 0 \qquad \text{on the boundary} \end{aligned}\right. \tag{3.8a}$$

$$\left.\begin{aligned} &\nabla \cdot h^{-1} \nabla \psi_\alpha = -\mu_\alpha \psi_\alpha \\ &h^{-1} \psi_\alpha = 0 \qquad \text{on the boundary*.} \end{aligned}\right. \tag{3.8b}$$

Here α is a binary index used for enumeration of the spectral components. These problems can now be shown to be self-adjoint. Hence, the characteristic values λ_α, μ_α are real and the characteristic functions ϕ_α, ψ_α each form a complete and internally orthogonal set. Since ϕ_α, ψ_α may be chosen as real without any loss of generality, the orthogonality statement may be written as:

$$\begin{aligned} &\int h^{-1} \mathbf{M}^{\phi}_{\alpha} \cdot \mathbf{M}^{\phi}_{\beta} \, dA = \lambda_\alpha \int \phi_\alpha \phi_\beta \, dA = C^2 A \bar{H}^2 \delta_{\alpha\beta} \\ &\int h^{-1} \mathbf{M}^{\psi}_{\alpha} \cdot \mathbf{M}^{\psi}_{\beta} \, dA = \mu_\alpha \int \psi_\alpha \psi_\beta \, dA = C^2 A \bar{H}^2 \delta_{\alpha\beta} \end{aligned} \tag{3.9}$$

*The factor h^{-1} in condition (3.8b) imposes a more stringent condition than required by (3.6). However, this is necessary to make (3.8b) self-adjoint.

Here $C^2 \equiv g\bar{H}$ and A is the surface area of the basin. $\delta_{\alpha\beta}$ is the Kronecker delta. In accordance with (3.3),

$$\mathbf{M}_\alpha^\phi = -\,h\,\nabla\,\phi_\alpha,\ \mathbf{M}_\alpha^\psi = -\,[\nabla\,\psi_\alpha] \tag{3.10}$$

were defined in the orthogonality statement (3.9).

Now the (non-dimensional) expansion coefficients are defined:

$$\begin{aligned} p_\alpha &\equiv \frac{1}{C^2\,A\,\bar{H}^2}\int h^{-1}\,\mathbf{M}_\alpha^\phi\cdot\mathbf{M}^\phi\,dA = \frac{1}{C^2\,A\,\bar{H}^2}\int h^{-1}\,\mathbf{M}_\alpha^\phi\cdot\mathbf{M}\,dA \\ q_\alpha &\equiv \frac{1}{C^2\,A\,\bar{H}^2}\int h^{-1}\,\mathbf{M}_\alpha^\psi\cdot\mathbf{M}^\psi\,dA = \frac{1}{C^2\,A\,\bar{H}^2}\int h^{-1}\,\mathbf{M}_\alpha^\psi\cdot\mathbf{M}\,dA \end{aligned} \tag{3.11}$$

to represent $\mathbf{M}^\phi$ and $\mathbf{M}^\psi$. In view of the orthogonality condition (3.9), the sums on the right of

$$\begin{aligned} \mathbf{M}^\phi &= \sum_\alpha p_\alpha\,\mathbf{M}_\alpha^\phi \\ \mathbf{M}^\psi &= \sum_\alpha q_\alpha\,\mathbf{M}_\alpha^\psi \end{aligned} \tag{3.12}$$

are least squares approximations to $\mathbf{M}^\phi$ and $\mathbf{M}^\psi$, when the sums span the complete spectra of (3.8a) and (3.8b) (with the usual restrictions on quadratic integrability and continuity of $\mathbf{M}^\phi$, $\mathbf{M}^\psi$, and their derivatives).

After orthogonal bases are established for $\mathbf{M}^\phi$ and $\mathbf{M}^\psi$, it now remains to obtain an appropriate basis for the height field ζ. From the continuity equation, it may be shown that ϕ_α forms a sufficient basis for ζ. For convenience

$$\zeta_\alpha \equiv C^{-1}\,(\lambda_\alpha)^{1/2}\,\phi_\alpha \tag{3.13}$$

The orthonormality relation among ζ_α is then

$$\int \zeta_\alpha\,\zeta_\beta\,dA = A\,\bar{H}^2\,\delta_{\alpha\beta}$$

The non-dimensional expansion coefficients are:

$$\gamma_\alpha \equiv \frac{1}{A\,\bar{H}^2}\int \zeta_\alpha\,\zeta\,dA \tag{3.14}$$

Pertaining to an expansion

$$\zeta = \sum_\alpha \gamma_\alpha\,\zeta_\alpha \tag{3.15}$$

In representations (3.12) and (3.15), the expansion coefficients p_α, q_α, γ_α are time-dependent. Associated with these expansions are the Parceval relations.

$$\begin{aligned} K^\phi &= \tfrac{1}{2}\,\rho\,(\bar{H})^{-1}\int h^{-1}\,(\mathbf{M}^\phi)^2\,dA = \tfrac{1}{2}\,M\,c^2\sum_\alpha p_\alpha^2 \\ K^\psi &= \tfrac{1}{2}\,\rho\,(\bar{H})^{-1}\int h^{-1}\,(\mathbf{M}^\psi)^2\,dA = \tfrac{1}{2}\,M\,c^2\sum_\alpha q_\alpha^2 \\ P &= \tfrac{1}{2}\,g\rho\int \zeta^2\,dA = \tfrac{1}{2}\,M\,c^2\sum_\alpha \gamma_\alpha^2 \end{aligned}$$

where $M \equiv \rho\, \bar{H} A$ is the mass of the fluid in the basin, K^{ϕ} and K^{ψ} are the kinetic energies associated with the irrotational and solenoidal parts of the flow field, and P is the potential energy.

By substituting the expansions (3.12) and (3.15) in the equations (2.1) and (2.2) with $\tau_S = 0$ and approximating τ_B by (2.5), then by isolating the spectral expansion coefficients, we obtain

$$\frac{d\,p_\alpha}{d\,t} + \lambda p_\alpha - f\sum_\beta A_{\alpha\beta}\, p_\beta - f\sum_\beta B_{\alpha\beta}\, q_\beta - \nu_\alpha \gamma_\alpha = 0^* \tag{3.16a}$$

$$\frac{d\,q_\alpha}{d\,t} + \lambda q_\alpha - f\sum_\beta C_{\alpha\beta}\, p_\beta - f\sum_\beta D_{\alpha\beta}\, q_\beta = 0^* \tag{3.16b}$$

$$\frac{d\,\gamma_\alpha}{d\,t} + \nu_\alpha p_\alpha = 0 \tag{3.16c}$$

Here the following definitions are introduced:

$$\begin{aligned} A_{\alpha\beta} &\equiv \left\{ \mathbf{M}^{\phi}_{\alpha}, [\mathbf{M}^{\phi}_{\beta}] \right\}, \quad B_{\alpha\beta} \equiv \left\{ \mathbf{M}^{\phi}_{\alpha}, [\mathbf{M}^{\psi}_{\beta}] \right\} \\ C_{\alpha\beta} &\equiv \left\{ \mathbf{M}^{\psi}_{\alpha}, [\mathbf{M}^{\phi}_{\beta}] \right\}, \quad D_{\alpha\beta} \equiv \left\{ \mathbf{M}^{\psi}_{\alpha}, [\mathbf{M}^{\psi}_{\beta}] \right\} \end{aligned} \tag{3.17}$$

where the notation $\left\{ \mathbf{A}, \mathbf{B} \right\}$ is used for

$$\left\{ \mathbf{A}, \mathbf{B} \right\} \equiv \frac{1}{C^2\, A\bar{H}^2} \int h^{-1}\, \mathbf{A} \cdot \mathbf{B}\, dA$$

which represents the inner product of the two vectors **A** and **B**. From (3.17) it can be seen that

$$A_{\alpha\beta} = -A_{\beta\alpha},\ B_{\alpha\beta} = -C_{\beta\alpha},\ D_{\alpha\beta} = -D_{\beta\alpha} \tag{3.18}$$

In equations (3.16a), (3.16b), and (3.16c) ν_α is given by

$$\nu_\alpha \equiv (c^2\, \lambda_\alpha)^{1/2} \tag{3.19}$$

and represents the normal mode frequency in the absence of rotation.

Now the column vectors are defined:

$$\vec{P} \equiv \mathrm{col}(p_\alpha), \quad \vec{Q} \equiv \mathrm{col}(q_\alpha), \quad \vec{R} \equiv \mathrm{col}(\gamma_\alpha) \tag{3.20}$$

$$\vec{S} \equiv \begin{pmatrix} \vec{P} \\ \vec{Q} \\ \vec{R} \end{pmatrix}$$

and the matrices

$$\mathbf{A} \equiv |A_{\alpha\beta}|\,,\ \mathbf{B} \equiv |B_{\alpha\beta}|\,,\ \mathbf{C} \equiv |C_{\alpha\beta}|\,,\ \mathbf{D} \equiv |D_{\alpha\beta}|$$

$$\langle \nu \rangle \equiv \text{diagonal}\ \nu_\alpha$$

*A more general friction law where $\lambda = \lambda\ (h)$ with $h = h(x,y)$ may be adopted than the one indicated by (2.5), if necessary. The only difference that would result in the spectral equations 3.16a and 3.16b is that the second term λp_α and λq_α on the left of each equation is replaced by $\sum_\beta \left\{ \lambda\ \mathbf{M}^{\phi}_{\alpha}, \mathbf{M}^{\phi}_{\beta} \right\} p_\beta$ and $\sum_\beta \left\{ \lambda\ \mathbf{M}^{\psi}_{\alpha}, \mathbf{M}^{\psi}_{\beta} \right\} q_\beta$, respectively.

Equations (3.16a), (3.16b), and (3.16c) may be written in the following form:

$$\frac{d\vec{S}}{dt} + a\vec{S} = 0 \tag{3.21}$$

where the square matrix a is defined as

$$a \equiv \left|\begin{array}{c|c|c} \lambda I^* - fA & -fB & -\langle\nu\rangle \\ \hline -fC & \lambda I - fD & 0 \\ \hline \langle\nu\rangle & 0 & 0 \end{array}\right| \tag{3.22}$$

If we assume that in (3.21)

$$\vec{S} \sim e^{-\sigma t}$$

then

$$(a - \sigma I)\,\vec{S} = 0$$

The values of σ are now the eigenvalues of the matrix a so that det. $|a\text{-}\sigma I| = 0$. These eigenvalues σ represent the normal mode frequencies for the rotating basin. The relations (3.18) and (3.21) show that a is an antisymmetric matrix. The associated eigenvectors then give the expansion coefficients p_α, q_α, γ_α. Use of these in (3.12) and (3.15) gives the $\mathbf{M}^\phi$ and $\mathbf{M}^\psi$ components of the transport vector **M** and the height field of the normal modes.

After the normal modes have been determined in the manner described above for an arbitrary basin, the procedure described in the next section can be used to construct the forced solution. It should be noted that obtaining the normal modes by solving the Neumann and Dirichlet problems (3.8a) and (3.8b) is much simpler than obtaining them by solving the problems posed by (3.1) and (3.2). The problems (3.8a) and (3.8b) for an arbitrary basin may be solved using Galerkin methods or a direct numerical finite-difference method. Application of this procedure to determine the normal modes for Lake Ontario will be discussed elsewhere.

4. FORCED SOLUTION

Various methods, as mentioned in the introduction, have been considered for the construction of the forced solution. These methods fall into two categories. One method gives a formal solution to the problem in terms of an integral over time for a set of either coupled or uncoupled equations. The other deals with finite-difference integration of the problem in time only.

In the formal solution two alternate procedures are given which differ only in the explicit details and which are labelled for convenience as *Method I* and *Method II.*

Method I

This method was used by Reid (1958) to study the edge wave resonance problem. Although this method may be developed with a linear, bottom friction law having a constant friction coefficient λ, this effect is ignored and $\vec{\tau}_B = 0$. Neglect of bottom friction is not such a drastic assumption, as it may seem at first, in the study of storm surge problems, which are transient in nature. During the

* I is the identity matrix.

transient stage when the wind stress force is acting on the surface, the effects of bottom friction will be an order of magnitude smaller. Hence, the neglect of the τ_B term in the equations, at least as a first approximation, can be justified.

The dynamic equations (2.1) and (2.2) are now considered. If $\tau_S = 0$ and $\mathbf{M}_F$ and ζ_F denote the normal modes or the free solutions, then they satisfy the equations

$$\frac{\partial \mathbf{M}_F}{\partial t} - f[\mathbf{M}_F] = -g\bar{H}h\nabla\zeta_F \tag{4.1}$$

$$\frac{\partial \zeta_F}{\partial t} + \nabla\cdot\mathbf{M}_F = 0 \tag{4.2}$$

satisfying the boundary condition (2.6).

In order to establish the normal mode functions, let

$$\mathbf{M}_F = \mathbf{M}_{j\alpha}(x,y)\,e^{i\,\sigma_j(\alpha)\,t} \tag{4.3}$$

$$\zeta_F = \zeta_{j\alpha}(x,y)\,e^{i\,\sigma_j(\alpha)\,t} \tag{4.4}$$

where $\mathbf{M}_{j\alpha}$, $\zeta_{j\alpha}$ are the space dependent normal mode functions and α is a wave number vector which represents the wave numbers in the x and y directions. For an arbitrary basin with variable bottom topography, for any given α, there are three allowable values of the frequency $\sigma_j(\alpha)$. These are designated as $\sigma_j(\alpha)$; $j = 1,2,3$ and denotes the two gravitational modes and one rotational mode such systems permit. For a basin with uniform depth, the spectrum of rotational modes is absent when the coriolis parameter is treated as a constant. Substitution of (4.3) and (4.4) into (4.1) and (4.2) yields the normal mode equations.

$$i\,\sigma_j(\alpha)\,\mathbf{M}_{j\alpha} - f[\mathbf{M}_{j\alpha}] = -g\bar{H}h\nabla\zeta_{j\alpha} \tag{4.5}$$

$$i\,\sigma_j(\alpha)\,\zeta_{j\alpha} + \nabla\cdot\mathbf{M}_{j\alpha} = 0 \tag{4.6}$$

The normal mode functions $\mathbf{M}_{j\alpha}$ and $\zeta_{j\alpha}$ are in general complex. A condition of orthogonality exists among these eigenfunctions in the generalized Hilbert sense and this may be deduced as follows.

If $\mathbf{M}^*_{k\beta}$, $\zeta^*_{k\beta}$ (the asterisk indicates a complex conjugate) are the normal mode functions associated with $\sigma^*_k(\beta)$, then the conjugate equations satisfied by these are:

$$-i\,\sigma^*_k(\beta)\,\mathbf{M}^*_{k\beta} - f[\mathbf{M}^*_{k\beta}] = -g\bar{H}h\nabla\zeta^*_{k\beta} \tag{4.7}$$

$$-i\,\sigma^*_k(\beta)\,\zeta^*_{k\beta} + \nabla\cdot\mathbf{M}^*_{k\beta} = 0 \tag{4.8}$$

Now multiply (4.5) by $\mathbf{M}^*_{k\beta}/g\bar{H}h$, (4.6) by $\zeta^*_{k\beta}$, (4.7) by $\mathbf{M}_{j\alpha}/g\bar{H}h$, (4.8) by $\zeta_{j\alpha}$, and add the resulting equations. The terms involving the coriolis parameter drop out. Integrating of the resulting expression over the area of the basin and using the boundary condition of vanishing normal component of the transport field yield the quadratic relation:

$$\left(\sigma_j(\alpha) - \sigma^*_k(\beta)\right)\int\left(\frac{\mathbf{M}_{j\alpha}\cdot\mathbf{M}^*_{k\beta}}{g\bar{H}h} + \zeta_{j\alpha}\zeta^*_{k\beta}\right)dA = 0$$

If $\sigma_j(\alpha) \neq \sigma^*_k(\beta)$ then the integral vanishes. If $j = k$, $\alpha = \beta$ then the integral does not vanish because the integrand is a sum of squares of real quantities. Consequently $\sigma_j(\alpha) = \sigma^*_j(\alpha)$, i.e., all eigenvalues are real. The condition of orthogonality among the eigenfunctions may then be stated as:

$$\int\left((\mathbf{M}_{j\alpha} \cdot \mathbf{M}^*_{k\beta})\,(g\,\bar{H}\,h)^{-1} + \zeta_{j\alpha}\,\zeta^*_{k\beta}\right)\,d\,A = X_{j\alpha}\,\delta_{jk}\,\delta_{\alpha\beta} \tag{4.9}$$

Here δ_{ij} is the Kronecker delta; $X_{j\alpha}$ represents the norm of the set of eigenfunctions and is closely related to the energy of the normal modes.

The set of normal mode functions and the associated frequencies form an essential part of the forced solution described by equations (2.1) and (2.2) (with $\tau_B = 0$), and explicit knowledge of these functions for the given basin is necessary. Assuming that the normal mode functions and their frequencies are known (this aspect was considered in the previous section), we may consider the solution to the forced problem to be of the form:

$$\mathbf{M}\,(x, y, t) = \sum_{j=1}^{3} \sum_{\alpha} A_{j\alpha}\,(t)\,\mathbf{M}_{j\alpha}\,(x, y) \tag{4.10}$$

$$\zeta\,(x, y, t) = \sum_{j=1}^{3} \sum_{\alpha} A_{j\alpha}\,(t)\,\zeta_{j\alpha}\,(x, y) \tag{4.11}$$

where $A_{j\alpha}$ is a complex time-dependent amplitude factor, which is closely related to the nature of the forcing function τ_S. The relationship between $A_{j\alpha}$ and $\dot{\tau}_S$ is obtained in the following way:

Substitute the solutions (4.10) and (4.11) into the governing equations (2.1) and (2.2) (with $\tau_B = 0$); multiply the momentum equations by $\mathbf{M}_{k\beta}\,/\,g\,\bar{H}\,h$ and the continuity equation by $\zeta^*_{k\beta}$; then take the conjugate equations (4.7) and (4.8) for the normal modes and multiply them by $\mathbf{M}\,/\,g\,\bar{H}\,h$ and ζ from (4.10) and (4.11), respectively. Add all the resulting equations and integrate over the area of the basin. Once again the coriolis terms drop out and use of the orthogonality condition (4.9) results in the following equation for $A_{j\alpha}$:

$$\frac{d\,A_{j\alpha}}{d\,t} - i\,\sigma_j\,(\alpha)\,A_{j\alpha} = B_{j\alpha} \tag{4.12}$$

$$B_{j\alpha} \equiv \frac{1}{X_{j\alpha}} \int \frac{\tau_S \cdot \mathbf{M}^*_{j\alpha}}{g\,\bar{H}\,h}\,dA$$

The preceding equation for $A_{j\alpha}$ is a simple ordinary inhomogeneous differential equation of the first order. Solution of this is

$$A_{j\alpha}\,(t) = \int_0^t B_{j\alpha}\,(\tau)\,e^{-i\,\sigma_j\,(\alpha)\,(\tau - t)}\,d\,\tau \tag{4.13}$$

which satisfies the initial conditions of the problem as given by equation (2.7).

From (4.12) it can be seen that $B_{j\alpha}$ represents simply the coefficients in the expansion of the forcing function τ_S in terms of the normal mode functions of the flow field. Hence, if the normal modes are known, $A_{j\alpha}$, which represents the time-dependent amplitudes of the normal modes, is obtained from (4.13) and the general solution of the forced problem, by going back to (4.10) and (4.11). In the preceding derivation, it may be noticed that the shape and bottom topography of the basin are left arbitrary. However, in practice, the crux of the entire matter lies in being able to solve (or already having knowledge of) the normal mode functions of the basin and their frequencies.

Method II

Going back to the procedure which yielded the spectral equations (3.16) for the free rotating problem, we follow the same steps except that τ_S is taken as a prescribed nonzero quantity. This leads to a system of inhomogeneous equations:

$$\frac{d\,p_\alpha}{d\,t} + \lambda\, p_\alpha - f \sum_\beta (A_{\alpha\beta}\, p_\beta + B_{\alpha\beta}\, q_\beta) - \nu_\alpha\, \gamma_\alpha = \left\{ \tau_S\ , M_\alpha^\phi \right\}$$

$$\frac{d\,q_\alpha}{d\,t} + \lambda\, q_\alpha - f \sum_\beta (C_{\alpha\beta}\, p_\beta + D_{\alpha\beta}\, q_\beta) = \left\{ \tau_S\ , M_\alpha^\psi \right\} \tag{4.14}$$

$$\frac{d\,\gamma_\alpha}{d\,t} + \nu_\alpha\, p_\alpha = 0$$

where $\left\{ \tau_S\ , M_\alpha^{\phi \text{ or } \psi} \right\}$ is defined as in (3.17). Comparison with (4.12) shows that the time-dependent problem now involves the solution to a coupled set of differential equations instead of the uncoupled set as obtained in (4.12). By defining another column vector:

$$\vec{F} \equiv \text{col} \begin{pmatrix} \left\{ \tau_S\ , M_\alpha^\phi \right\} \\ \left\{ \tau_S\ , M_\alpha^\psi \right\} \\ 0 \end{pmatrix} \tag{4.15}$$

To represent the forcing function, equations (4.14) may be cast into the following form:

$$\frac{d\vec{S}}{d\,t} + a\,\vec{S} = \vec{F} \tag{4.16}$$

Here $\vec{S}$ and a are the same as those defined in (3.20) and (3.22). Equation (4.16) represents an ordinary inhomogeneous differential equation of the first order in the matrix form. Matrix a is time-independent and contains the essence of the natural characteristics of the basin and may be computed once and for all.

The solution of (4.16) may be obtained by the usual integrating factor method and may be written as

$$\vec{S} = e^{-a\,t} \int_0^t e^{a\tau}\, \vec{F}\,(\tau)\, d\,\tau \tag{4.17}$$

where the meaning of the exponential matrix is as follows. If σ values are the characteristic values of the matrix a, then using the theory of similarity transformations produces

$$a = \tilde{c} < \sigma > \tilde{c}^{-1} \tag{4.18}$$

where $<\sigma>$ is a diagonal matrix of the characteristic values and $\tilde{c}$ is a modal matrix containing the eigenvectors arranged in columns. The exponential matrices e^{at} and e^{-at} are now given by

$$e^{a\,t} = \tilde{c}\ < e^{\sigma\, t} >\ \tilde{c}^{-1}$$

$$e^{-a\,t} = \tilde{c}\ < e^{-\sigma\, t} >\ \tilde{c}^{-1}$$

Using these in (4.17) gives

$$\vec{S} = \tilde{c}\ < e^{-\sigma\, t} >\ \tilde{c}^{-1} \int_0^t \tilde{c}\ < e^{\sigma\,\tau} >\ \tilde{c}^{-1}\ \vec{F}\ (\tau)\ d\,\tau$$

as the formal solution for the time-dependent amplitudes of the forced problem. The expression above can be further simplified to give

$$\vec{S} = \tilde{\mathbf{c}} \; \langle e^{-\sigma t} \rangle \int_0^t \langle e^{\sigma \tau} \rangle \; \tilde{\mathbf{c}}^{-1} \; \vec{F} \; (\tau) \; d\tau \tag{4.19}$$

The integral then may be evaluated by any of the standard methods of integration.

Finite difference integrations

Finally, a direct numerical integration of the ordinary differential-matrix equation (4.16) or (4.12) may be considered by using any of the various available finite difference schemes (Baer and Simons, 1970), either explicit or implicit. These schemes may be written as follows: equation (4.16) as

$$\frac{d\vec{S}}{dt} = \vec{g} \; (\vec{S}, \vec{F}, t) \tag{4.20}$$

The general finite-difference extrapolation formulae may be written as follows (using the notation of Baer and Simons):

(a) explicit schemes: E_{pn}

$$\vec{S}^{t+\Delta t} = \vec{S}^{t-p\Delta t} + \Delta t \sum_{j=0}^{n} \bar{\alpha}_{E_j} \vec{g}^{t-j\Delta t} \tag{4.21}$$

(b) implicit schemes: I_{pn}

$$\vec{S}^{t+\Delta t} = \vec{S}^{t-p\Delta t} + \Delta t \sum_{j=0}^{n} \bar{\alpha}_{I_j} \vec{g}^{t+(1-j)\Delta t} \tag{4.22}$$

In the above expressions,

$$\bar{\alpha}_{E_j} \; (p) \equiv \int_{-p}^{1} \alpha_{E_j} \; (S) \; ds, \qquad \bar{\alpha}_{I_j} \; (p) \equiv \int_{-p}^{1} \alpha_{I_j} \; (S) \; dS$$

$$\alpha_{E_j} \; (S) \equiv \binom{-S}{j} \sum_{k=0}^{n-j} (-1)^k \binom{-S-j}{k}$$

$$\alpha_{I_j} \; (S) = \binom{-S+1}{j} \sum_{k=0}^{n-j} (-1)^k \binom{-S-j+1}{k}$$

The parameter p is an integer representing a point in time $(t - p\Delta t)$ at which the function $\vec{g}$ is known; n represents an integer giving the time $(t - n\Delta t)$ at which the oldest value of the function $\vec{g}$ is known; the symbol $\binom{S}{j}$ is a binomial coefficient function of s.

The finite-difference integration in time may be carried out for any scheme (chosen by giving appropriate values for p and n) in a straightforward manner. This still has an advantage over a complete finite-difference integration of the governing partial differential equations of the problem, which requires a three-dimensional space-time grid. Further, as (4.16) is a linear system of equations, the implicit integration procedures can be used, which do not impose any limits on time increments. By using an Euler trapezoidal method (obtained by putting $p = 0$ and $n = 1$)

we get

$$\bar{\alpha}_{I_0} = \frac{1}{2} = \bar{\alpha}_{I_1}$$

and the use of scheme (4.22) on equation (4.16) then yields:

$$\vec{S}^{t+1} = \left(\frac{2I}{\Delta t} + a\right)^{-1} \left(\frac{2I}{\Delta t} - a\right) \vec{S} + \left(\frac{2I}{\Delta t} + a\right)^{-1} (\vec{F}^{t+1} + \vec{F}^{t}) \tag{4.23}$$

With this procedure, the matrix inversion of $\left(\frac{2I}{\Delta t} + a\right)$ needs to be done only once and the matrix multiplication on the right can be done once and for all for a given basin (using some fixed value of Δt). Application of the implicit integration procedure to equation (4.12) results in a simpler equation than (4.23) and is given by

$$\vec{A}^{t+1} = \left\langle \frac{2 - i\,\sigma_j\,(\alpha)\,\Delta t}{2 + i\,\sigma_j\,(\alpha)\,\Delta t} \right\rangle \vec{A}^{t} + \left\langle \frac{\Delta t}{2 + i\,\sigma_j\,(\alpha)\,\Delta t} \right\rangle \left(\vec{B}^{t+1} + \vec{B}^{t}\right) \tag{4.24}$$

where $\vec{A}$ represents the column $(A_{j\alpha})$ and $< >$ represents a diagonal matrix. Although there is no limit on the value of Δt used in these methods, it is well known that the Euler trapezoidal method gives large phase errors if Δt is larger than about one-sixth of a period of the fastest wave in the system. (Kurihara, 1965).

Summarizing the discussions in Sections 3 and 4 shows that a procedure has been developed through which the normal mode frequencies and structures may be determined for an arbitrary basin. By using these normal mode structures, the forced response is obtained by solving equations that give the time-dependence of the normal mode excitations. The integrations involved in the procedure, such as the ones in (4.12) and (4.14), can be done by Simpson's or trapezoidal rules of integration. These rules determine the inhomogeneous terms in these equations. The time-dependent behaviour of the amplitudes is obtained either from (4.13) or (4.19) by using the same procedure to evaluate the integrals, or by solving the system by a finite-difference integration as, for example, indicated in (4.23) and (4.24). As the normal modes must be calculated only once for a given basin, several of the quantities involved here can be stored for repeated use in future calculations. It is also obvious from the preceding considerations that the most advantageous method for operational purposes will be method I leading to equation (4.12), which is then solved by the implicit scheme given by equation (4.24).

Examples of Forced Oscillations

The application of the theory described above to some ideal cases is discussed, specifically, for the following problems.

A. Response of a non-rotating rectangular basin of uniform depth to a disturbance propagating across the basin with a given speed and making a certain angle to the north-south direction. Because the effects of rotation are ignored, the results are applicable only to those cases where the time-scale of the phenomenon is less than the local inertia period. In view of this short time-scale, bottom friction effects are also ignored here.

B. Response of a rotating rectangular basin of uniform depth to a stationary wind stress. Bottom friction is taken into account here through a linear frictional law.

Some of the details of the results for the two cases above will now be presented and discussed.

A. DISTURBANCE PROPAGATING OVER A NON-ROTATING BASIN OF UNIFORM DEPTH

5. NORMAL MODES

A rectangular basin ($-a \leqslant x \leqslant a$, $0 \leqslant y \leqslant b$) with uniform depth, so that $h = 1$ for this case, is considered. As rotation is ignored (as well as bottom friction), the normal mode solutions are:

$$
\begin{aligned}
M_{j\alpha} &= \frac{g\bar{H}}{i\,\nu_j(\alpha)} \cdot \frac{k\pi}{2a} \sin \frac{k\pi}{2a}(x+a) \cos \frac{l\pi y}{b} \\
N_{j\alpha} &= \frac{g\bar{H}}{i\,\nu_j(\alpha)} \frac{l\pi}{b} \cos \frac{k\pi}{2a}(x+a) \sin \frac{l\pi y}{b} \\
\zeta_{j\alpha} &= \cos \frac{k\pi}{2a}(x+a) \cos \frac{l\pi y}{b}
\end{aligned}
\tag{5.1}
$$

where it is assumed that the normal mode functions corresponding to the height-field have unit amplitude. In terms of the theory described in Section 3, the flow field in the absence of rotation contains only the irrotational component; the solutions in (5.1) may be considered as the solutions of the Neumann problem (3.8a). The binary index α represents (k,l) where k and l may take on any integral value between 0 and ∞. The frequencies of the normal modes are given by

$$
\nu_j^2(\alpha) = g\bar{H}\pi^2 \left(\frac{k^2}{4a^2} + \frac{l^2}{b^2}\right) \tag{5.2}
$$

As the rotational part of the flow field is zero in the case of non-rotation, the spectrum of possible modes contains only the gravitational modes.

6. FORCED SOLUTION

To obtain the forced response the procedure is used which was described as Method I in Section 4. The norm $X_{j\alpha}$ of the eigenfunctions (defined in (4.9)) is calculated from (5.1) and is given by

$$X_{j\alpha} = \epsilon_\alpha \, a \, b$$

where

$$\epsilon_\alpha \equiv \begin{cases} 1 & \text{if } k \, . \, l \neq 0 \\ 2 & \text{if } k \, . \, l = 0 \end{cases}$$

As the gravity modes occur in pairs with $\nu_1\ (\alpha) = -\ \nu_2\ (\alpha)$ (as seen from (5.2)), the following properties are also obtained

$$M_{1\alpha} = M_{2\alpha}^{*} \,,\ N_{1\alpha} = N_{2\alpha}^{*} \,,\ \zeta_{1\alpha} = \zeta_{2\alpha}^{*} \,,\ A_{1\alpha} = A_{2\alpha}^{*} \tag{6.1}$$

As noted above, the rotational mode spectrum is evanescent for this case. Hence the summation over j for the forced solutions (4.10 and 4.11) only goes from j = 1 to j = 2. In view of (6.1), the solutions may be explicitly written as:

$$\begin{aligned} M &= 2 \,\mathrm{Re} \sum_\alpha - \frac{i g \bar{H} k \pi}{2 a \nu_\alpha} A_\alpha (t) \sin \frac{k \pi}{2 a} (x + a) \cos \frac{l \pi y}{b} \\ N &= 2 \,\mathrm{Re} \sum_\alpha - \frac{i g \bar{H} l \pi}{b \nu_\alpha} A_\alpha (t) \cos \frac{k \pi}{2 a} (x + a) \sin \frac{l \pi y}{b} \\ \zeta &= 2 \,\mathrm{Re} \sum_\alpha A_\alpha (t) \cos \frac{k \pi}{2 a} (x + a) \cos \frac{l \pi y}{b} \end{aligned} \tag{6.2}$$

On the right hand sides of (6.2), Re indicates that the real part of the expression should be taken. The expansion coefficients A_α (t) are to be determined from (4.13) where B_α (t) is to be calculated from the following expression:

$$\begin{aligned} B_\alpha (t) = \frac{i}{\epsilon_\alpha \nu_\alpha ab} \int \Big[& \tau_{sx} (x, y, t) \frac{k \pi}{2 a} \sin \frac{k \pi}{2 a} (x + a) \cos \frac{l \pi y}{b} \\ & + \tau_{sy} (x, y, t) \frac{l \pi}{b} \cos \frac{k \pi}{2 a} (x + a) \sin \frac{l \pi y}{b} \Big] dA \end{aligned} \tag{6.3}$$

where τ_{sx} , τ_{sy} are the scalar components of the surface stress vector $\boldsymbol{\tau}_S$. B_α (t) from (6.3) can be evaluated once $\boldsymbol{\tau}_S$ is prescribed as a function of x,y,t.

If a step function stress field $\boldsymbol{\tau}_S$ propagates across the basin with speed V and at an angle θ measured clockwise from the north, then

$$|\boldsymbol{\tau}_S| = \begin{cases} 0 & \text{for } \gamma \geqslant Vt \\ \boldsymbol{\tau}_0 & \text{for } \gamma \leqslant Vt \end{cases} \tag{6.4}$$

where $\boldsymbol{\tau}_0$ is some scale value of the stress and $\gamma \equiv [(x + a)^2 + y^2]^{1/2}$ if $0 \leqslant \theta \leqslant \pi/2$. $\theta = 0$ or $\pi/2$ represent a step function approaching the basin from the south or west, respectively, and if $0 < \theta < \pi/2$, the forcing function approaches the basin from the SW quadrant (Fig. 1). If $\theta = 0$ or $\pi/2$, the problem simply reduces to a one-dimensional response of the basin and can be solved exactly using, for example, the method of characteristics (Rao, 1967).

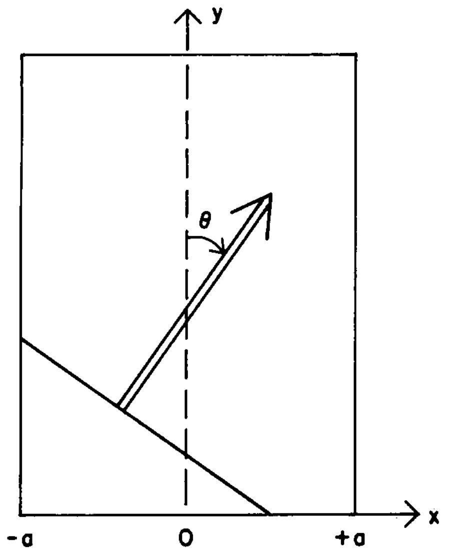

Figure 1
A schematic diagram of the rectangular basin with the stress band approaching from an angle θ.

The space integration for B_α in (6.3) then covers only that part of the basin over which the forcing function is non-zero. During the transient stage when the step-function is crossing the basin with $0 \leqslant \theta \leqslant \pi/2$, various epochs of time must be distinguished as shown in Figure 2, which then determine the domain of integration. The disturbance is assumed to be semi-infinite.

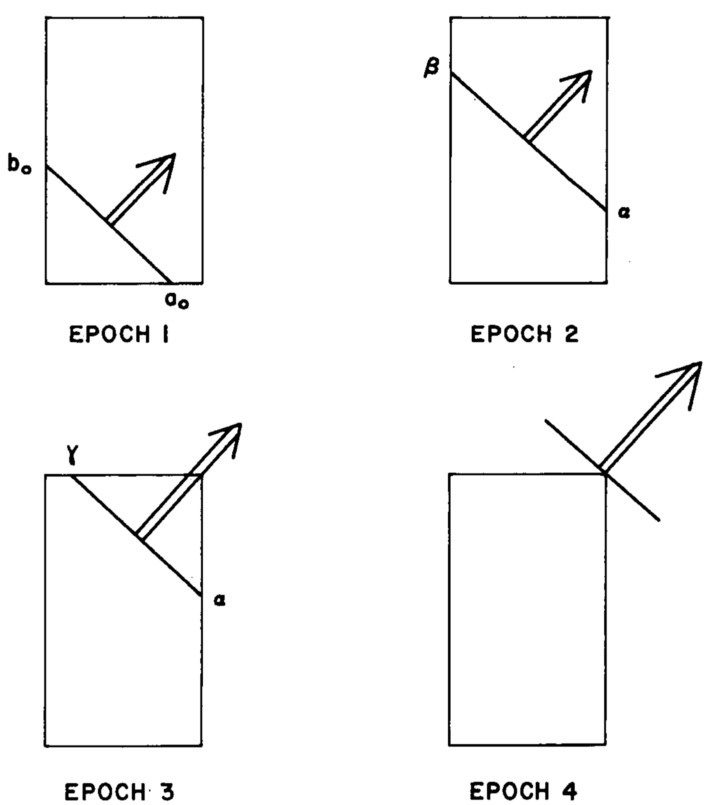

Figure 2
Various epochs of time as the stress band crosses the basin.

(i) During epoch 1, the forcing is acting only in the part of the basin given by $-a \leqslant x \leqslant (Vt \operatorname{cosec} \theta - a)$ and $0 \leqslant y \leqslant (a_0 - x) \tan \theta$ where $a_0 \equiv (Vt \operatorname{cosec} \theta - a)$. Epoch 1 comes to an end when $a_0 = a$ or $Vt_1 \operatorname{cosec} \theta = 2a$.

(ii) Epoch 2 starts at time $t \geqslant t_1$. The domain of integration may be split into two parts. One covers the area $-a \leqslant x \leqslant a$ and $0 \leqslant y \leqslant \alpha$, $\alpha \equiv Vt \sec \theta - 2a \tan \theta$. This is the same as Epoch 1 applied at $t = t_1$. The second part covers the area $-a \leqslant x \leqslant a$ and $\alpha \leqslant y \leqslant \left[\frac{(\beta + \alpha)}{2} - \frac{(\beta - \alpha)x}{2a}\right]$ where $\beta = Vt \sec \theta$. Epoch 2 ends at t_2 given by $Vt_2 \sec \theta = b$.

(iii) Epoch 3 begins for $t \geqslant t_2$. The area of integration is now split into three parts: $-a \leqslant x \leqslant a$, $0 \leqslant y \leqslant \alpha$; $-a \leqslant x \leqslant \gamma$, $\alpha \leqslant y \leqslant b$ $[\gamma \equiv (Vt \sec \theta - a \tan \theta - b) / \tan \theta]$ and $\gamma \leqslant x \leqslant a$, $\alpha \leqslant y \leqslant [(b - \alpha)\, x + (\gamma\alpha - ab)] / (\gamma - a)$. Epoch 3 ends at time t_3 given by $Vt_3 = (4a^2 + b^2)^{1/2}$.

(iv) After $t \geqslant t_3$, the entire basin is under the influence of forcing and the domain of integration covers $-a \leqslant x \leqslant$ and $0 \leqslant y \leqslant b$. The preceding regimes of time are for the cases where $Vt_1 \operatorname{cosec} \theta = 2a$ but $Vt_1 \sec \theta < b$. But, depending upon θ, a, and b, situations may exist where at time t_1, $Vt_1 \operatorname{cosec} \theta < 2a$ while $Vt_1 \sec \theta = b$. Then during epoch 1, the integration domain is the same as the one given earlier. Now epoch 2 is different and the domain of integration for $B_\alpha(t)$ covers $(-a \leqslant x \leqslant \gamma, 0 \leqslant y \leqslant b)$ and $[\gamma \leqslant x \leqslant a_0, 0 \leqslant y \leqslant b\,(a_0 - x) / (a_0 - \gamma)]$. Epoch 2 now ends at t_2 given by $Vt_2 \operatorname{cosec} \theta = 2a$. After $t = t_2$, the integration domain is identical to the previous ones. It is a straightforward matter to evaluate the quantity B_α using the limits of integration above and hence $A_\alpha(t)$. We shall dispense with writing the explicit formulas here since they are long and tedious.

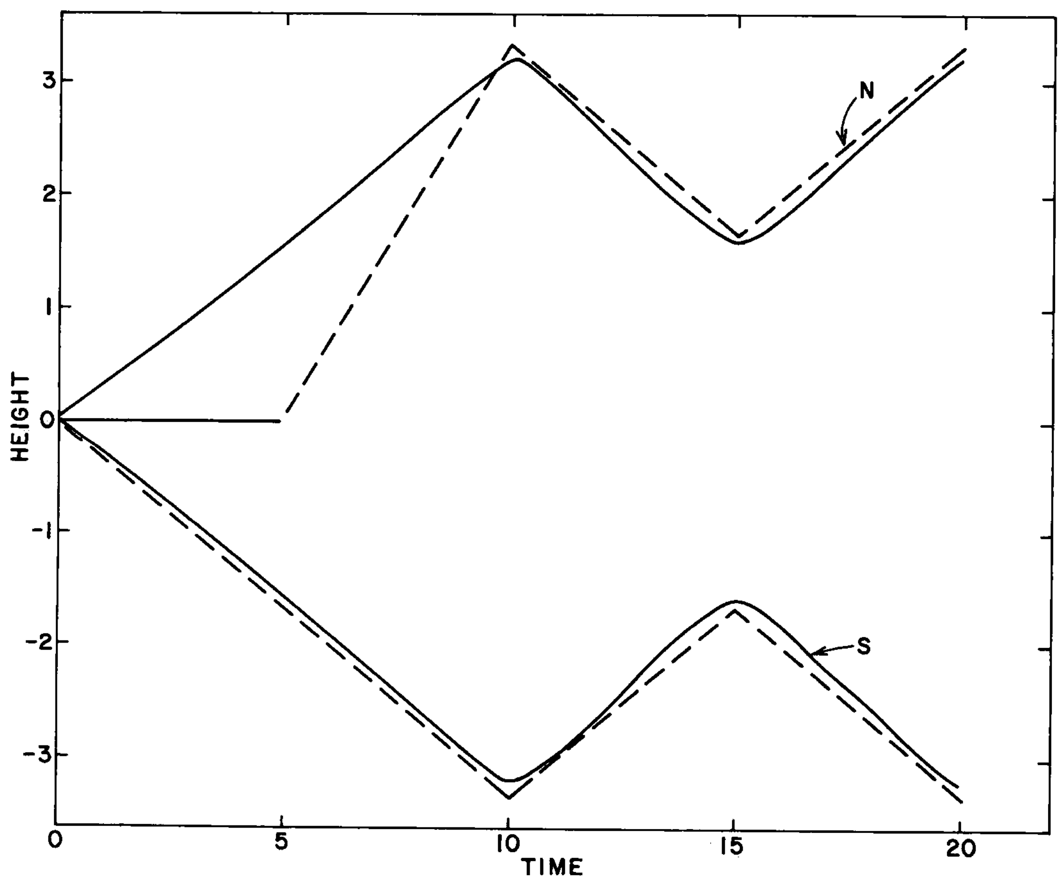

Figure 3. Comparison of spectral solution (solid line) with the exact solution (dashed line) for $\theta = 0$, $V = 0.5$, and $b/a = 5$.

Before B_α (t) and A_α (t) can be explicitly evaluated, the wave-numbers ($k\pi/2a$, $l\pi/b$) or rather (k, l) must be ordered in some manner with respect to the binary index. This ordering is arbitrary. However, because the lowest modes are more excited than the higher modes when a forcing function has a horizontal scale equal to, or larger than, the scale of the basin, the ordering is done in such a manner that the frequencies ν_α form an ascending sequence with respect to α that is

$$\nu_1 < \nu_2 < \nu_3 \;\; \dots \; .$$

7. RESULTS

Because a basin of uniform depth on a non-rotating plane was considered, it would suffice to calculate the response for values of θ restricted to one quadrant, which was chosen here as $0 \leqslant \theta \leqslant \pi/2$. The results will be presented for the height field ζ at a few points on the boundary as a function of time for several speeds of propagation V and direction of approach θ of the disturbance. Height field and time t are made non-dimensional according to:

$$\zeta \rightarrow \frac{c^2 \zeta}{\tau_0 \, a} \; , \; t \rightarrow \frac{c\,t}{a}$$

where $c \equiv \sqrt{g\,H}$ is the speed of free long gravity waves on the surface. The speed of propagation V of the disturbance is also made non-dimensional ($V \rightarrow V/c$).

Figure 3 shows a comparison of the spectral solution for a basin of elongation $b/a = 5.0$ with $V = 0.5$ and $\theta = 0$ against the exact solution. As $\theta = 0$, the disturbance is propagating northwards along the basin and the response here simply reduces to a one-dimensional case. The exact solution for this case – that is, the solution obtained by summing (6.2) over the infinity of normal modes – is given by Rao (1967). This is indicated by the dashed line in Figure 3 whereas the spectral solution summed over the lowest ten normal modes is given by the solid line. The solutions on the southern boundary (S) agree very well for all time and on the northern boundary (N) from $t \geqslant 10$. During $0 < t < 10$, the spectral solution differs from the exact solution on the northern boundary. This is due to the fact that the period $0 < t < 10$ represents the transient stage when the stress band is crossing the basin. The northern boundary will stay undisturbed until the first free gravity wave arrives there, which happens at $t = 5$. Then the water level starts to rise until the forced wave arrives at $t = 10$. Such discontinuous behaviour, as is well known, cannot be represented by the spectral methods. Even though the details of the water level on the northern boundary during the transient period are poorly represented, however, the maxima and minima of the water level fluctuations and the times of their occurrence are very well predicted by the spectral method with only a few components.

Figures 4-7 show the water fluctuations at the four corners of a square basin. Figures 4 and 5 represent the case when $V = 0.5$ and $\theta = \pi/6$ and $\pi/3$, respectively. Figures 6 and 7 represent the case when $V = 1.5$ and $\theta = \pi/6$ and $\pi/3$, respectively. In all cases the height field is calculated in time up to $t = 2t_3$, where t_3 represents the time at which the stress band completely traversed the entire basin. The four corners at which the results are shown are labelled LL (lower left), LR (lower right), UL (upper left), and UR (upper right). In this notation then t_3 represents the time at which the forced wave arrives at the upper right corner. A glance at these diagrams shows the complicated nature of the two-dimensional response. In the one-dimensional case, the maximum water level on the opposite boundary (to the point where the stress band starts its propagation at the initial time) always occurs at the instant when the slower of the two waves – free and forced – arrives at the boundary. If a basin of length 2 in the one-dimensional case is considered, the minimum water levels are obtained on the boundary at which the stress band starts. Time of occurrence of the minimum values is given by $t = 2(1+ V^{-1})$ if $V^{-1} \leqslant 1$, $t = 4$ if $1 \leqslant V^{-1} \leqslant 2$ and if $2 \leqslant V^{-1} \leqslant \infty$ the minimum values are obtained at $t =$

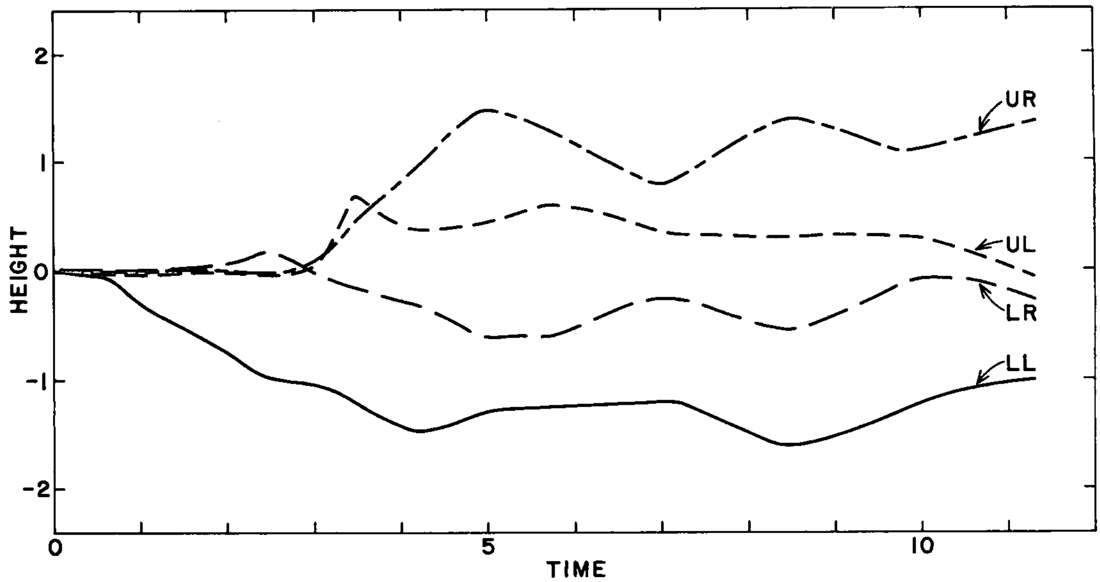

Figure 4. Water level fluctuations at points x = −a, y = 0 (LL); x = a, y = 0 (LR); x = −a, y = b (UL); x = a, y = b (UR); as a function of time for $\theta = \pi/6$, V = 0.5 in a square basin.

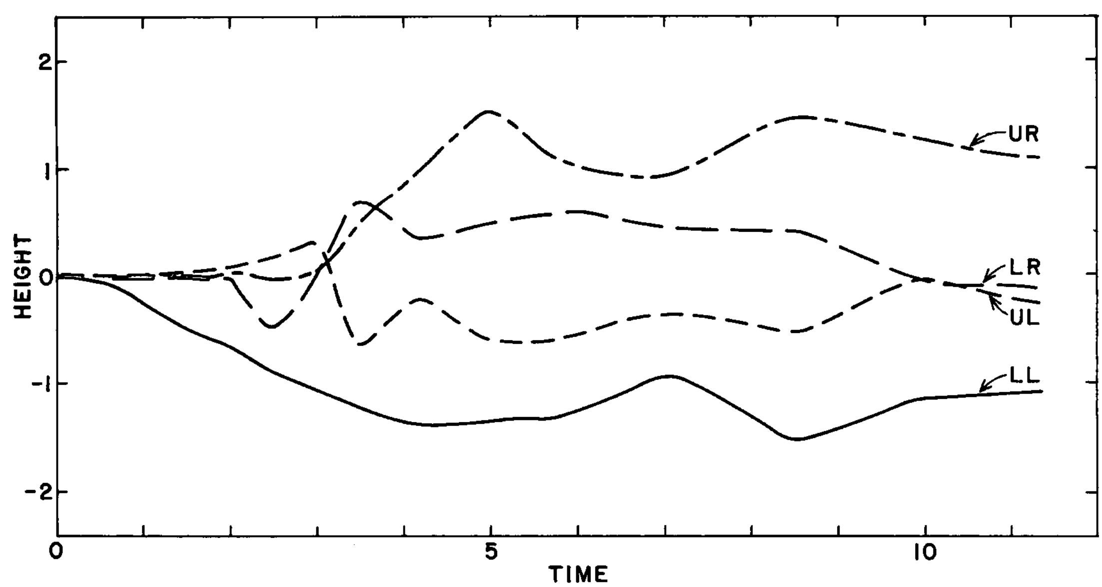

Figure 5. Water level fluctuations at points x = −a, y = 0 (LL); x = a, y = 0 (LR); x = −a, y = b (UL); x = a, y = b (UR); as a function of time for $\theta = \pi/3$, V = 0.5.

$2V^{-1}$ for V^{-1} even and $2(V^{-1} - 1)$ for V^{-1} odd. Such properties no longer hold for the two-dimensional case even if the length is now defined as the diagonal length. In Figs. 6 and 7, it appears as if the maximum values on the northeast (upper right) corner are obtained at $t \approx 2.8$, which will be the time required for a free gravity wave to traverse the diagonal of a square basin having sides of length 2. This is, indeed, what the one-dimensional theory predicts for the case $V > 1$. However, the occurrence of the maximum at $t \approx 2.8$ is only fortuitous and such behaviour is generally found to be not true.

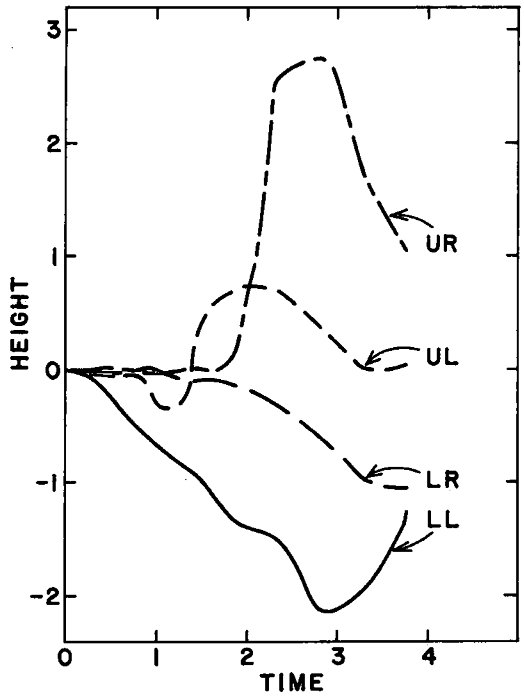

Figure 6
Water level fluctuations at points $x = -a, y = 0$ (LL); $x = a, y = 0$ (LR); $x = -a, y = b$ (UL); $x = a, y = b$ (UR); as a function of time for $\theta = \pi/6$, $V = 1.5$.

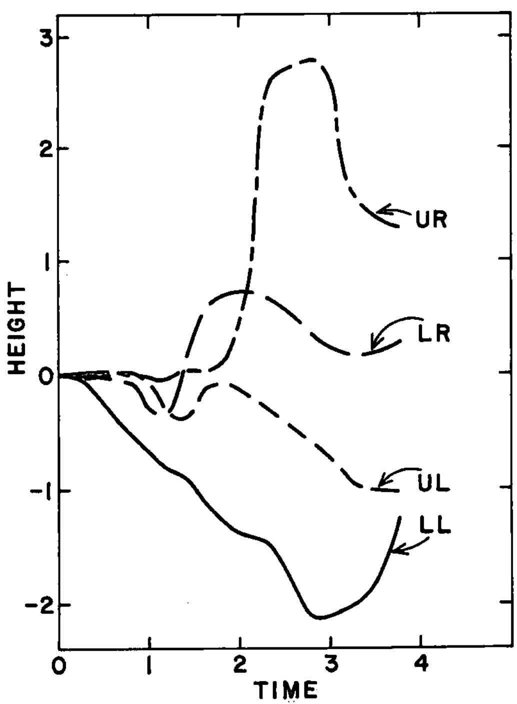

Figure 7
Water level fluctuations at points $x = -a, y = 0$ (LL); $x = a, y = 0$ (LR); $x = -a, y = b$ (UL) $x = a$, $y = b$ (UR); as a function of time for $\theta = \pi/3$, $V = 1.5$.

The nature of the two-dimensional response is complicated due to the multiple reflections obtained in the basin. As a result each corner exhibits several oscillations with different maxima and minima and no periodicity appears to exist even after the transient period is over and the entire basin is under the influence of constant forcing. From the calculations performed for $0 \leqslant \theta \leqslant \pi/2$, it appears, however, that the highest water levels are obtained at the northeast corner and the lowest at the southwest corner. The peak values are tabulated for a few cases in Tables 1 and 2. Table 1 gives the maximum and minimum water levels in a square basin for various speeds of propagation and two directions of approach ($\theta = \pi/6, \pi/3$) of the disturbance. Table 2 gives data for a basin whose length in y-directions is two and a half times the length in the x-direction. An inspection of the tables shows that the maximum water levels seem to be obtained for a speed of propagation V centered about 1.25. Furthermore, there appears to be a tendency for the magnitudes of maximum and minimum water levels to reach some constant values for speeds $V > 1.75$. Qualitatively this property is similar to the one-dimensional case where the maxima and minima on the appropriate boundaries are independent of the speed of propagation when $V \geqslant 1$. The results given here are for the case of a semi-infinite stress as pointed out earlier. Results for a finite width stress band may be obtained from these by graphical super-position of the solutions. The solutions may also be obtained theoretically by prescribing the forcing function (6.4) for a finite band width.

Table 1. Maximum (at the northeast corner) and minimum (at the southwest corner) water levels as a function of V and θ for a square basin

V	$\theta = \pi/6$		$\theta = \pi/3$	
	Max.	Min.	Max.	Min.
0.25	1.2	-1.2	1.3	-1.4
0.5	1.4	-1.4	1.5	-1.5
0.75	2.3	-2.0	2.4	-2.0
1.0	2.9	-2.1	2.9	-2.2
1.25	3.3	-2.0	3.5	-2.1
1.5	2.8	-2.2	2.8	-2.1
1.75	2.9	-2.2	3.0	-2.3
2.0	2.9	-2.2	3.0	-2.3

Table 2. Maximum (at the northeast corner) and minimum (at the southwest corner) water levels as a function of V and θ for a basin having north-south length two and a half times the east-west length

V	$\theta = \pi/6$		$\theta = \pi/3$	
	Max.	Min.	Max.	Min.
0.25	2.4	-2.4	2.3	-1.9
0.5	3.2	-3.2	3.4	-2.5
0.75	4.3	-3.6	4.5	-2.8
1.0	3.8	-3.2	5.7	-2.9
1.25	5.2	-4.3	5.4	-3.4
1.5	4.4	-4.2	5.0	-3.6
1.75	4.3	-3.7	3.9	-2.9
2.0	4.3	-3.6	3.9	-2.8

B. STATIONARY DISTURBANCE OVER A ROTATING BASIN OF UNIFORM DEPTH

8. CONSTRUCTION OF THE ORTHOGONAL FUNCTIONS

In the rotating case the normal modes are built up from the solutions of (3.8a) and (3.8b). When the depth of the basin is assumed to be a constant h = 1, and if the geometry is once again taken to be rectangular with $0 \leqslant x \leqslant a$ and $0 \leqslant y \leqslant b$, the solutions for ϕ_α and ψ_α are:

$$\phi_\alpha = \epsilon_\alpha C \bar{H} \lambda_\alpha^{-1/2} \cos \frac{k \pi x}{a} \cos \frac{l \pi y}{b}$$

$$\psi_\alpha = 2 C \bar{H} \mu_\alpha^{-1/2} \sin \frac{k \pi x}{a} \sin \frac{l \pi y}{b}$$

$$\lambda_\alpha = \mu_\alpha = \pi^2 \left(\frac{k^2}{a^2} + \frac{l^2}{b^2} \right) \tag{8.1}$$

$$\epsilon_\alpha \equiv \begin{cases} \sqrt{2} & \text{if } k \cdot l = 0 \\ 2 & \text{if } k \cdot l \neq 0 \end{cases}$$

The amplitudes of ϕ_α and ψ_α are chosen so as to satisfy the orthonormality condition (3.9). The matrix coefficients $A_{\alpha\beta}$ etc., may now be evaluated and are given by

$$A_{\alpha\beta} = \frac{4 \epsilon_\alpha \epsilon_\beta}{A \sqrt{\lambda_\alpha \lambda_\beta}} \left\{ \frac{k_\beta^2 l_\alpha^2 - k_\alpha^2 l_\beta^2}{(k_\alpha^2 - k_\beta^2)(l_\alpha^2 - l_\beta^2)} \right\}$$

$$B_{\alpha\beta} = - \frac{8 \epsilon_\alpha}{\pi^2} \sqrt{\frac{\lambda_\alpha}{\mu_\beta}} \frac{k_\beta l_\beta}{(k_\alpha^2 - k_\beta^2)(l_\alpha^2 - l_\beta^2)} = - C_{\beta\alpha} \tag{8.2}$$

The coefficients $D_{\alpha\beta}$ are all zero for this case. The formulae given in (8.2) are only valid under the restriction that

$$k_\alpha - k_\beta \text{ is odd}$$

$$l_\alpha - l_\beta \text{ is odd}$$

If this condition is not met,

$$A_{\alpha\beta} = B_{\alpha\beta} = C_{\alpha\beta} = 0$$

9. FORCED SOLUTION

The forced solutions are presented only for the case of a stationary, time-independent disturbance. Then the forcing terms in (4.15) are given by

$$\int \tau_S \cdot M_\alpha^\phi \, dA = \frac{2\sqrt{2} C \bar{H}}{\sqrt{\lambda_\alpha}} \begin{cases} b\, \tau_{S_x} & \text{if } l_\alpha = 0, k_\alpha \text{ is odd} \\ a\, \tau_{S_y} & \text{if } k_\alpha = 0, l_\alpha \text{ is odd} \end{cases}$$

$$\int \tau_S \cdot M_\alpha^\psi \, dA = 0 \text{ for all } (k_\alpha, l_\alpha) \tag{9.1}$$

The quantities τ_{S_x} and τ_{S_y} are constants.

Here also the wave-number ordering is done in such a manner that the no-rotation frequencies ν_α form an ascending sequence of numbers. The response is solved using Method II previously described, and for this special case of constant forcing, the solution (4.19) can be written as

$$\vec{S} = (I - \widetilde{C} < e^{-\sigma t} > \widetilde{C}^{-1})\ a^{-1}\ \vec{F} \tag{9.2}$$

If n terms each are taken in the expansions (3.12) and (3.15) (note that each of the series for $\mathbf{M}^\phi$, $\mathbf{M}^\psi$, and ζ may be truncated at different numbers of terms, if desired), the column vector $\vec{S}$ has 3n elements and the matrix a is of the order 3n x 3n. Hence there are 3n eigenvalues, or normal mode frequencies. These correspond to 2n gravity modes and n viscous modes.* The 2n gravity modes consist of n complex frequencies, which represent the frequencies modified by rotation and n of their conjugates. After collecting the elements p_α, q_α, and γ_α (9.2), the forced solutions for $\mathbf{M}^\phi$, $\mathbf{M}^\psi$, and ζ are obtained from (3.12) and (3.15), and the total transport field **M** from the condition $\mathbf{M} = \mathbf{M}^\phi + \mathbf{M}^\psi$. These solutions in component form may be stated as follows.

$$M(x, y, t) = C \bar{H} \pi \, \mathrm{Re} \sum_{i=1}^{n} \left\{ \sum_{j=1}^{3n} \left[(\alpha_j \widetilde{C}_{ij}\, e^{-\sigma_j t} + x_i)\, \epsilon_i\, k_i \right.\right.$$
$$\left.\left. - 2(\alpha_j \widetilde{C}_{i+n,j}\ e^{-\sigma_j t} + x_{i+n})\, l_i \frac{a}{b} \right] \cdot \left(k_i^2 + \frac{a^2}{b^2}\, l_i^2\right)^{-1/2} \cdot \sin \frac{k_i \pi_x}{a} \cos \frac{l_i \pi_y}{b} \right\} \tag{9.3}$$

$$N(x, y, t) = C \bar{H} \pi \, \mathrm{Re} \sum_{i=1}^{n} \left\{ \sum_{j=1}^{3n} \left[(\alpha_j \widetilde{C}_{ij}\, e^{-\sigma_j t} + x_i)\, \epsilon_i\, l_i \frac{a}{b} \right.\right.$$
$$\left.\left. + 2(\alpha_j \widetilde{C}_{i+n,j}\ e^{-\sigma_j t} + x_{i+n})\, k_i \right] \cdot \left(k_i^2 + l_i^2 \frac{a^2}{b^2}\right)^{-1/2} \cos \frac{k_i \pi x}{a} \sin \frac{l_i \pi y}{b} \right\}$$

$$\zeta(x, y, t) = \pi \bar{H}\, \mathrm{Re} \sum_{i=1}^{n} \epsilon_i \left(\sum_{j=1}^{3n} \alpha_i \widetilde{C}_{i+2n,j}\ e^{-\sigma_j t} + x_{i+2n} \right) \cdot \cos \frac{k_i \pi_x}{a} \cos \frac{l_i \pi_y}{b}$$

where α_j and x_j are the elements of the column vectors

$$\vec{\alpha} \equiv \mathrm{col}\,(\alpha_j) = -\widetilde{C}^{-1}\,(a^{-1}\,\vec{F})$$

and

$$\vec{x} \equiv \mathrm{col}\,(x_j) = a^{-1}\,\vec{F}$$

The results computed from formulae above are given in the following section in terms of the height field ζ.

10. RESULTS

Results obtained for the response of a rectangular basin of uniform depth to a stationary disturbance are presented. The basin is rotating at constant angular speed of rotation and a constant linear bottom friction in the problem is retained. Two specific cases are presented: (a) a high rotation with large friction; and (b) a low rotation with small friction. In either case, the basin is taken as a 2 x 1 rectangle, i.e., a/b = 2; and a steady wind stress acting in the positive x-direction only is

*These are induced by the presence of the bottom friction term and consequently represent a set of damped modes.

considered so that in (9.1)

$$\tau_{sx} = \tau_0 = \text{constant}$$

$$\tau_{sy} = 0$$

The results are once again presented in terms of non-dimensional numbers. The non-dimensionalization is now expressed as follows:

$$f \to f/\nu_1 \ , \ t \to \nu_1 t \ , \ \lambda \to \lambda/\nu_1$$

where $\nu_1 = C\pi/a$ is the frequency of the lowest, longitudinal no-rotation mode. Hence the non-dimensional time $t = 2\pi$ represents the period of oscillation of the slowest no-rotation mode. The non-dimensional height field is given in terms of

$$\zeta \to \sqrt{2} \ \pi^2 \ \frac{C^2 \zeta}{a \tau_0}$$

where τ_0 is a scale value of the wind stress.

The orthogonal functions (8.1) used to build up the normal modes (and the forced solution) have either symmetric or antisymmetric properties. That is,

$$F(a - x \ , \ b - y) = F(x, y) \qquad \text{(symmetric)}$$

$$F(a - x \ , \ b - y) = - F(x, y) \quad \text{(antisymmetric)}$$

where F can be either ϕ_α or ψ_α. This property of symmetry and antisymmetry for ϕ_α and ψ_α is governed by the rule:

$k_\alpha + l_\alpha$ is odd (antisymmetric)

$k_\alpha + l_\alpha$ is even (symmetric)

For the simple case considered here, there is no coupling between symmetric and antisymmetric parts, which means that the matrix coefficients $A_{\alpha\beta}$, $B_{\alpha\beta}$, and $C_{\alpha\beta}$ are zero if α and β represent symmetric and antisymmetric wave-number pairs, respectively, or vice versa. Also, since any contribution to the forcing function (9.1) is excluded from a symmetric wave-number pair, all symmetric modes are omitted in the wave-number ordering of the binary index α. The antisymmetric modes are then arranged so that the ν_α form an ascending sequence.

A convergence test is made for the forced response for the high rotation with large friction case. The series for M and ζ are truncated once at ten terms each and next at fifteen terms each. The convergence question is examined in terms of the sum of the squares of the expansion coefficients $(\sum_\alpha |p_\alpha|^2 + |q_\alpha|^2 + |\gamma_\alpha|^2)$, which represents the length of the column vector $\vec{S}$. After a time $t = 4\pi$ (time corresponding to two no-rotation periods), the difference in the solutions between the two truncations is of the order of 2%. For earlier time periods, the convergence is better.

Consider now the response for the high rotation with large friction case. Numerical values chosen for this case are

$$f = 2 \ , \ \lambda = 0.2$$

The results are given in Figure 8 which shows the time variation of the water levels at three points on the boundary. These points are labelled as lower right (LR), which represents the point with the coordinates x=a, y = 0; center right (CR) with the coordinates x = a, y = b/2; and upper right (UR) with the coordinates x = a, y = b. These coordinates are indicated on the inset diagram in Figure 8. In the upper part of Figure 8 is given the water level variation at the point x = a/2, y = 0. The variations of the height fields at diagonally opposite points on the boundary are simply given by the negative values at each of the corresponding points in view of the antisymmetric nature of the solutions. Also given in Figure 8 is the response curve on the boundary x = a for the no-rotation case for purposes of comparison.

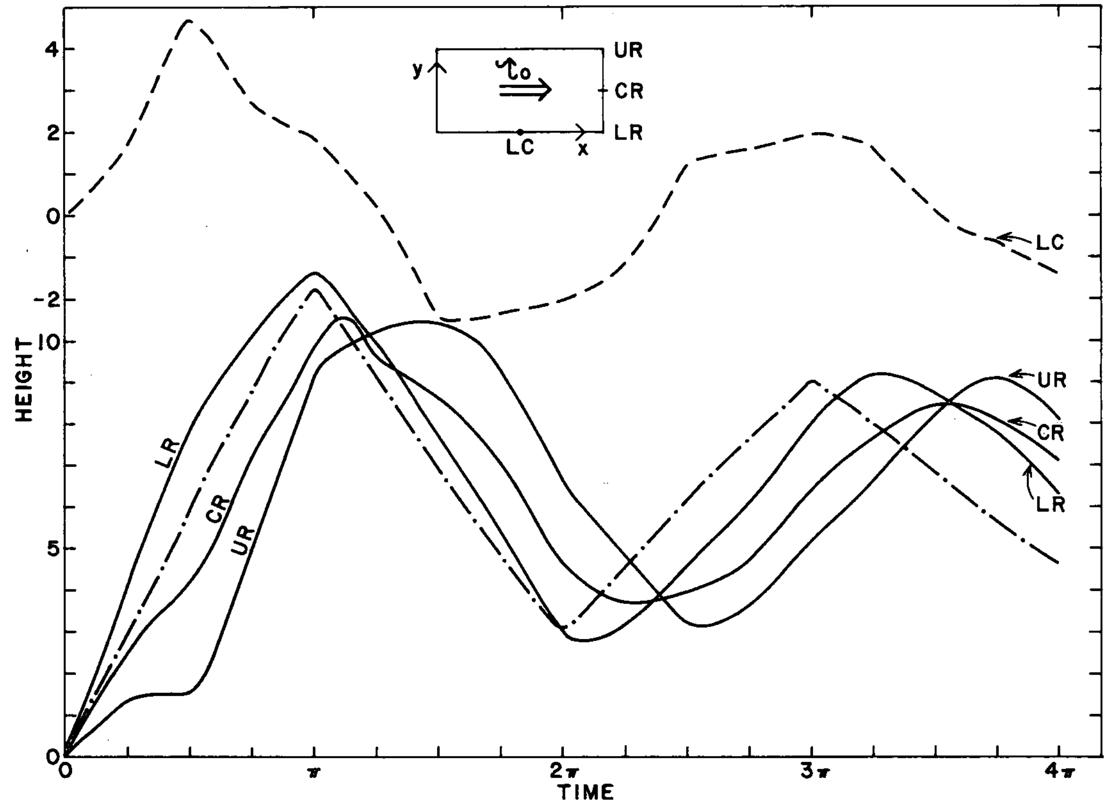

Figure 8. Water level fluctuations *vs.* time at various points on the boundary of a rotating rectangular basin. These points are located on the inset diagram of a rectangle along with the direction of wind stress. In this picture, f = 2, b/a = 0.5, λ = 0.2. The non-rotational response is given by the dashed line and is valid at all points of the side x = a.

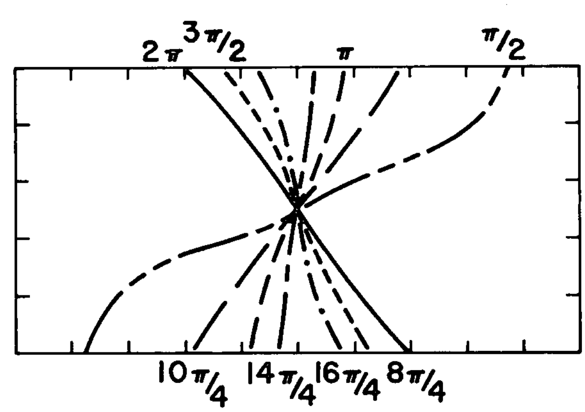

Figure 9
Location of the nodal line in the (x,y)-plane at various instants of time for parameter values given in Figure 8.

It is shown in Figure 8 that, when rotation is taken into account, the maximum water level is first obtained in the lower right corner of the basin, which is obviously due to the rightward deflection of the water body in reaction to the coriolis forces. The maximum obtained at the point labelled LR is larger than the corresponding value obtained when rotation is ignored. The high-water level then proceeds northward along the eastern edge of the basin where the subsequent peak values obtained at points CR and UR are somewhat smaller. This may be due to the fairly high value assigned to the coefficient of friction here. The height fields reach minimum values at different times as shown in Figure 8. If there were no rotation and no friction, the fluctuation of water level on the eastern boundary ($x = a$) would be such that it would reach a maximum at $t = \pi$ and zero at $t = 2\pi$ for the instantaneously imposed wind field considered here (see Rao, 1967). The presence of rotation and/or friction will prevent the water level from returning to zero value at any subsequent time after the initial instant. If the solution is carried out over a long period, the transient effects produced by the normal modes in (9.2) would damp out and the solution would asymptotically approach the steady state value. The influence of rotation is also evident from the upper diagram in Figure 8, corresponding to the changes in height field at the point LC. If rotation is absent, the water level will have a zero value for all time at this point as it coincides with the position of the stationary nodal line obtained in such a case. When rotation is taken into account, the nodal line is no longer fixed in space for all time, and the height field at LC deviates from zero as indicated.

Figure 9 shows the position of the nodal line in the (x, y)-plane at various instants in time. As seen from (9.2), the general solution consists of the particular solution corresponding to the forcing and a contribution from the homogeneous (normal mode) solutions. In the initial stages, when the water level is building up under the influence of forcing, the high water moves in a clockwise sense

Table 3. Height values (cm) on the southern boundary from spectral and finite-difference methods at approximately $t = 0.5$ T.

x	Spectral (cm)	Finite-difference (cm)
0	−1.15	−1.12
1/20	−1.11	
1/12		−0.98
2/20	−0.99	
3/20	−0.85	
2/12		−0.83
4/20	−0.72	
5/20 or 3/12	−0.61	−0.60
6/20	−0.50	
4/12		−0.38
7/20	−0.37	
8/20	−0.24	
5/12		−0.20
9/20	−0.12	
10/20 or 6/12	+0.004	+0.009
11/20	0.11	
7/12		0.21
12/20	0.24	
13/20	0.37	
8/12		0.40
14/20	0.49	
15/20 or 9/12	0.61	0.64
16/20	0.72	
10/12		0.87
17/20	0.85	
18/20	0.99	
11/12		1.02
19/20	1.12	
20/20 or 12/12	1.16	1.15

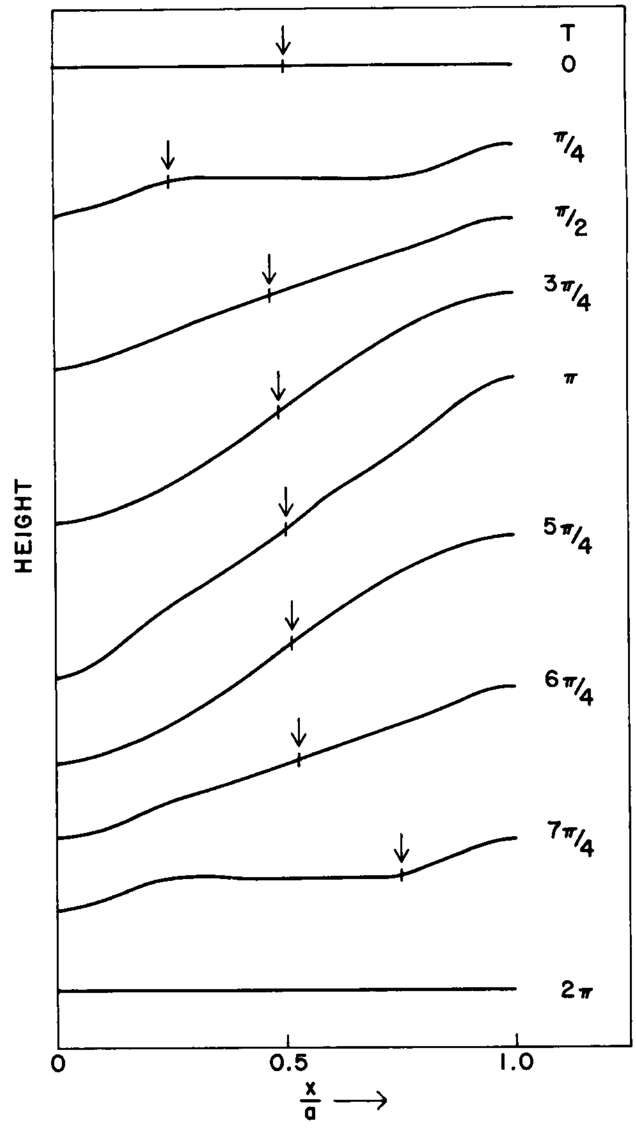

Figure 10. Water level fluctuations on the southern boundary ($y = 0$) as a function of time for $f = 0.12$, $\lambda = 10^{-2} \times f$, $b/a = 0.5$ with a uniform wind stress in the positive x-direction.

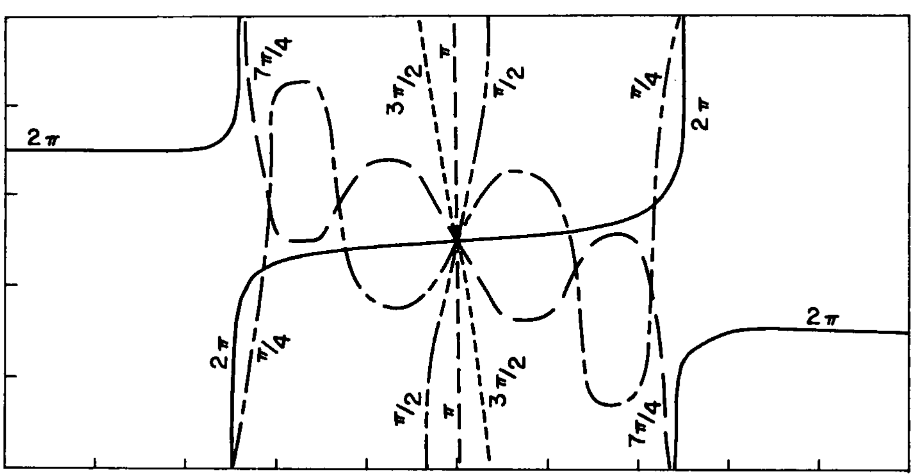

Figure 11. Nodal line configuration at various instants of time for parameter values given in Figure 10.

along the north and south boundaries (that is, along $y = b$ and $y = 0$ boundaries), due to the inertial effects of rotation. After approximately $t = \pi/2$, the nodal line (and hence the high water) starts to travel in a counter-clockwise direction. This effect is produced by the slowest rotating normal mode, that is, the non-rotating fundamental longitudinal mode transformed by the effects of rotation. In the individual contributions of the normal modes to the general solution, the slowest mode is the dominant one, as can be seen from the spectral decomposition; this mode is characterized by a counter-clockwise propagation of the nodal line, which then accounts for the behaviour described above. The influence of the fundamental mode persists up to approximately $t = 2\pi$, when the forced solution once again starts to build up resulting in a rapid clockwise shift of the nodal line as evidenced by the shift of this line from $t = 2\pi$ to $t = 10\pi/4$. The cycle of counter-clockwise propagation once again starts after $t = 10\pi/4$ in the same manner as described above.

The case of low rotation with small friction is considered next. The values chosen are $f = 0.12$ and $\lambda = 10^{-2}f$. This case has been run to compare the solution obtained by the spectral method with the one obtained by T. J. Simons (personal communication) using finite difference integrations. For a value of $\rho^{-1}\tau_0 = 1\ cm^2\ s^{-2}$, the dimensional values of ζ from both methods are compared in Table 3. The height field is given for various values of x on the southern boundary. The spectral solution for truncation of series at fifteen terms is given at $t = T/2$ or π (T is the no-rotation period of the fundamental longitudinal mode) and the finite-difference solution is that at $t = 7/15\ T$; this difference in time at which the solutions are obtained should be rather insignificant. The comparison as can be seen by an inspection of the values listed in the table is favourable.

Figure 10 shows schematically the change in water level along the southern boundary, at various instants in time over an interval corresponding to one period of oscillation of the no-rotation slowest longitudinal mode. The location of the nodal line on the southern boundary is indicated by an arrow. The initial shift of the nodal line in the clockwise direction is followed by a counter-clockwise propagation of the nodal line. One can see the influence of higher harmonics in the response in this case of low rotation with small friction. This is made more clear by an inspection of Figure 11, which shows the nodal line in the (x, y)-plane at various instants in time. Between $t = \pi/2$ to $3\pi/2$, the nodal line configuration shows the dominance of the slowest rotating mode, and for $t > 3\pi/2$ and $t < \pi/2$, the response is dominated by higher rotating modes.

Summary

The general theory for obtaining the forced response of an arbitrary water body by using the normal modes of the basin was discussed. Use of the normal modes in the representation of the forced solution eliminates the space dependent aspect of the problem which then reduces the original partial differential equations governing the forced response to a set of ordinary time-dependent inhomogeneous differential equations. These equations determine the normal mode excitations by the forcing field. A procedure for determining the normal modes for quasi-static motions in an arbitrary water body including rotation and bottom friction was discussed along with a few different methods of constructing the forced response. Application of these methods to two simple cases was then considered. One case dealt with a semi-infinite stress band which propagates at an angle to the north-south direction along a rectangular basin of uniform depth. Rotation and bottom friction are ignored in this case. The second case considered the response of a rotating rectangular basin of uniform depth to an instantaneously imposed wind stress of constant strength. Bottom friction is taken into account through a simple frictional law. Results for these two examples were presented. In both these cases, the method of using the normal modes was found to be satisfactory, and work is now in progress in applying these methods to real geophysical water bodies, e.g., the Great Lakes.

References

BAER, F. and T. J. SIMONS. 1970. Computational stability and time-truncation of coupled nonlinear equations with exact solutions. *Monthly Weather Review,* 98, 665-679.

KURIHARA, Y. 1965. On the use of implicit and iterative methods for the time-integration of the wave equation. *Monthly Weather Review,* 98, 33-46.

LAMB, H. 1932. *Hydrodynamics,* 6th edition. Cambridge University Press, 738 pp.

LAUWERIER, H. A. 1961. The North Sea problem IV. Non-stationary wind effects in a rectangular bay. (Theoretical part). Proceedings, *Koninklijke Nederlandske Akademie Van Wetenschappen, Series A,* 64, 104-122.

LAUWERIER, H. A. and B. R. DAMSTE. 1963. The North Sea Problem VIII. A numerical treatment. *Proceedings, Koninklijke Nederlandske Akademie Van Wetenschappen, Series A,* 66, 167-184.

LOOMIS, H. G. 1970. A method of setting up the eigenvalue problem for the linear, shallow water wave equation for irregular bodies of water with variable water depth and application to bays and harbors in Hawaii. *Hawaii Inst. Geophysics HIG-70-32,* 9 pp.

PLATZMAN, G. W. 1963. The dynamical prediction of wind tides on Lake Erie. *Meteorological Monographs,* 4, No. 26, 44 pp.

PLATZMAN, G. W. 1971. Two-dimensional free oscillations in natural basins. Dept. Geophysical Sciences, Univ. Chicago, Rep. No. 23, 106 pp.

PLATZMAN, G. W. and D. B. RAO. 1964. The free oscillations of Lake Erie. Studies on Oceanography. Univ. Washington Press, 359-382.

PROUDMAN, J. 1916. On the dynamical theory of tides. Part II. Flat seas. *Proceedings, London Mathematical Society, 2nd Series,* 18, 21-50.

PROUDMAN, J. 1929. The effects on the sea of changes in atmospheric pressure. *Mon. Not. Roy. Astron. Soc., Geophys. Suppl.,* 2, 197-209.

RAO, D. B. 1966. Free gravitational oscillations in rotating rectangular basins. *Journal of Fluid Mechanics,* 25, 523-555.

RAO, D. B. 1967. Response of a lake to a time-dependent wind stress. *Journal of Geophysical Research,* 72, 1697-1708.

RAO, D. B. 1969. Effect of travelling disturbances on a rectangular bay of uniform depth. *Arch. Met. Geoph. Biokl., Ser,A,* 18, 171-190.

REID, R. O. 1958. Effect of coriolis force on edge waves. (1) Investigation of normal modes. *Journal of Marine Research,* 16, 109-141.

SIMONS, T. J. 1971. Development of numerical models of Lake Ontario. *Proceedings, 14th Conference on Great Lakes Research,* Toronto, Ont., April 19-21, 1971. Intl. Assoc. Great Lakes Research, pp. 654-669.

WELANDER, P. 1961. Numerical prediction of storms surges. *Advances in Geophysics,* 8, 316-379.